Synthesis and biological evaluation of carbamates derived from aminocombretastatin A-4 as vascular disrupting agents

Laura Conesa-Milián,[a] *Eva Falomir,* [a]* *Juan Murga,* [a]* *Miguel Carda,*[a] *Eef Meyen,*[b] *Sandra Liekens,*[b] *J. Alberto Marco*[c]

[a]Depart. de Q. Inorgánica y Orgánica, Univ. Jaume I, E-12071 Castellón, Spain

[b]Depart. of Microbiology and Immunology, KU Leuven, Rega Institute for Medical Research, Herestraat 49, B-3000 Leuven, Belgium

[c]Depart. de Q. Orgánica, Univ. de Valencia, E-46100 Burjassot, Valencia, Spain

*Authors to whom correspondence should be addressed. E-Mail address: jmurga@uji.es, efalomir@uji.es

ABSTRACT

A series of twenty-six carbamates derived from aminocombretastatin A-4 (AmCA-4) were synthesized and evaluated for their capacity to affect cell proliferation, tubulin polymerization, mitotic cell arrest, microtubule network organization, apoptosis and endothelial tubular structures in vitro. The anti-proliferative activity of the synthetic carbamates was measured on several human tumor cell lines (i.e. HT-29, MCF-7, HeLa, A-549, MDA-MB-231, HL-60) as well as on the endothelial cell line HMEC-1 and the non-tumor cell line HEK-293. The compounds showed anti-proliferative activity in the nanomolar range thereby exceeding by far the activity of combretastatin A-4 (CA-4) and, in some cases, the activity of AmCA-4. The most active compounds proved to be the carbamates bearing chloro, bromo or methoxy groups in the *meta* position of the phenyl ring. Moreover, all carbamates inhibited in vitro tubulin polymerization, in a similar manner to that of CA-4 and AmCA-4 by interacting with the colchicine binding site in tubulin. The synthetic carbamates proved as active as AmCA-4 in causing mitotic arrest, as assessed in A549 human lung cancer cells, and disruption of the microtubule cellular network. Some selected carbamates induced apoptosis at concentrations as low as 10 nM, being more active than AmCA-4. Finally, these selected carbamates displayed a vascular disrupting activity on endothelial cells in a dose-dependent manner. In conclusion, our data indicate

that carbamates derived from aminocombretastatin A-4 represent interesting lead compounds for the design of vascular disrupting agents.

KEYWORDS
Tubulin, aminocombretastatin, microtubules, carbamates, vascular disrupting agents, apoptosis.

1. Introduction

The tumor vasculature supplies oxygen and nutrients to the fast-growing tumor cells and removes toxic metabolites from the tumor site. However, this vascular network is highly disordered, tortuous and unstable due to the lack of proper regulation of the angiogenic process [1].The high density of abnormal intratumoral blood vessels allows cancer cells to easily gain access to the blood thus triggering the metastasis process. Blocking the tumor vasculature is thus an alternative approach to traditional radio- and chemotherapy in the fight against cancer. There are two main approaches to achieve this goal either by preventing new blood vessel formation (i.e. anti-angiogenic agents) or by directly destroying the tumor vasculature. Vascular disrupting agents (VDAs) are compounds that selectively damage the unstable tumor vasculature thus causing tumor ischemia and necrosis.

One class of VDAs, that includes the well-studied colchicine and combretastatin A-4, exerts their action by binding to tubulin, the protein that forms the cytoskeletal microtubules. This binding destroys the cellular structural framework and disrupts intercellular junctions, leading to loss of morphology and cohesion of tumor vascular endothelial cells and to subsequent collapse of the tumor vasculature [2]. Combretastatin A-4 (CA-4), a natural phenolic stilbene which has been isolated from the African willow tree Combretum caffrum (see figure 1), is a potent anti-mitotic agent against a variety of cancer cells, including multi-drug resistant cancer cell lines [3]. CA-4 also acts on proliferating endothelial cells [4] and displays vascular disrupting action [5]. The poor water solubility of CA-4 has prevented its use as an anticancer drug which explains the development of phosbretabulin, a water-soluble

prodrug of CA-4 that also shows potent antivascular and antitumor effects in a wide variety of tumor cell lines [6]. In the last years several VDAs, such as combretastatin A-4 phosphate (Phosbretabulin disodium salt), AVE8062 (Ombrabulin), DMXAA (Vadimezan), NPI-2358 (Plinabulin) and MPC-6827 have entered phase 2-3 trials (see figure 1) [7].

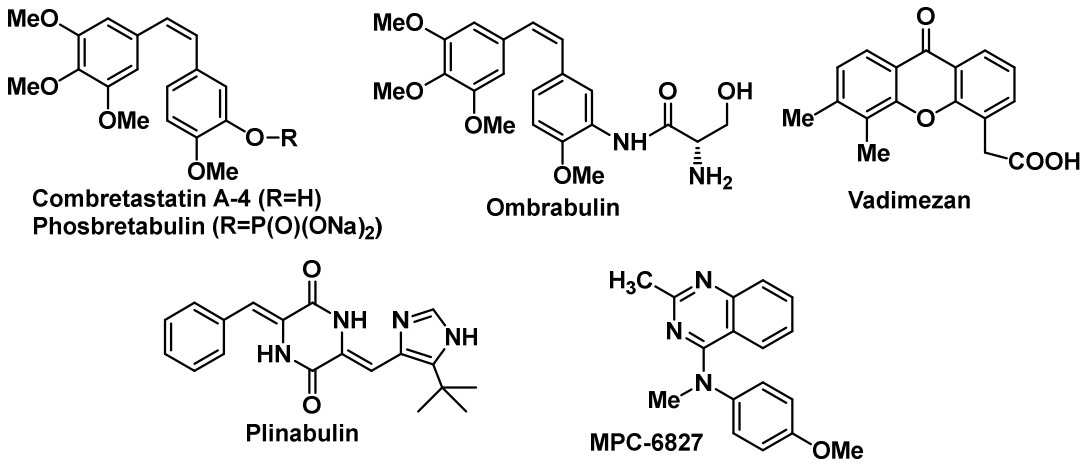

Figure 1.

The poor water solubility of CA-4 has prevented its use as an anticancer drug which explains the development of aminocombretastatin (AmCA-4), a non-natural combretastatin, and Ombrabuline, a serine-derivative from AmC4-4 (see figure 2). These compounds also show strong cytotoxicity, inhibition of tubulin polymerization and antivascular activity [8].

Several drugs exhibit a carbamate group in their structures as in rivastigmine (used for the treatment of dementia), retigabine (prescribed for the treatment of epilepsies), morizicine (used for the treatment of arrhythmias), zafirlukast (used for the treatment of asthma), and as in antiretroviral drugs used for the treatment of HIV/AIDS, like efavirenz, ritonavir, darunavir, fosamprenavir, atazanavir and cobicistat. Carbamate functionality confers chemical and proteolytic stability and a great capacity to pass through cell membranes which explains the increasing use of carbamates in medicinal chemistry [9]. The delocalization of nonbonded electrons of nitrogen over the carboxyl moiety causes a

conformational rigidity. In addition, the NH and the carboxyl group exhibit excellent capacities for the formation of hydrogen bonds. Thus, substitution on the *N*- and *O*-termini of a carbamate allows to fine-tune the biological and pharmacokinetic properties of carbamate-bearing molecules.

In particular, the *cis*-stilbene structural fragment of CA-4 can be considered as a privileged motif with regard to VDA activity [10]. Figure 2 depicts a compound in which aminocombretastatin A-4 and a functionalized phenol have been linked through the intermediacy of a carbamate group.

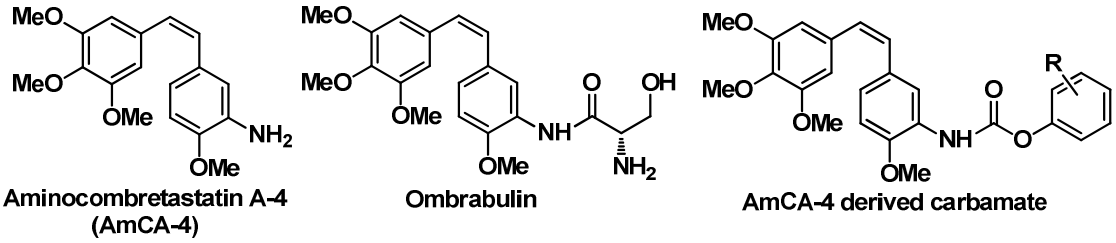

Figure 2.

2. Research purpose

During the past few years we have been investigating a range of analogues of natural products for their potential value in anticancer therapy [11]. We have published several reports on the biological properties of combretastatin A-4 derivatives [12]. Therefore, on the basis of the aspects commented above and in continuation of our research on novel natural product analogues with potential utility in cancer therapy, we wanted to study whether carbamoylation of the amino group in aminocombretastatin A-4 improves its biological activity [13]. The synthesis of this new family of combretastatin-derived carbamates is described in scheme 1. The structures of the synthesized carbamates are indicated in figure 3.

3. Synthetic work

Aminocombretastatin was prepared by total synthesis following a published procedure [14]. For the synthesis of carbamates two procedures were applied. In the indicated *Method a* in scheme 1

carbamates were directly achieved upon reaction of AmCA-4 with commercially available aryl chloroformates in THF in the presence of pyridine [15]. The low commercial availability of aryl chloroformates allowed only the synthesis of three carbamates with the application of *Method a* (compounds **1**, **4** and **7**, see figure 3). The remaining carbamates were prepared by one-pot *Method b* in which AmCA-4 was converted into the corresponding trichloromethylcarbamate, upon reaction with triphosgene and Et_3N, which in turn was transformed into carbamates by reaction with a range of phenols (see scheme 1) [16].

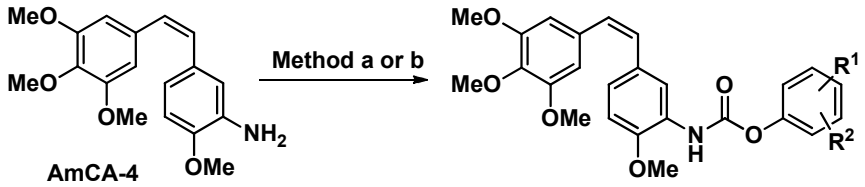

Scheme 1. Reagents and conditions**:** Method a: ArOCOCl, pyridine, THF, 0ºC 30 min then rt 1 h. Method b: (i) Triphosgene, Et_3N, THF, rt, 10 min; (ii) ArOH, THF, 45ºC, 1 h.

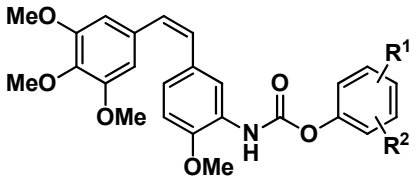

1 (R^1, R^2=H, method a , 89%)
2 (R^1=2-F, R^2=H, method b, 73%)
3 (R^1=3-F, R^2=H, method b, 33%)
4 (R^1=4-F, R^2=H, method a , 64%)
5 (R^1=2-Cl, R^2=H, method b, 35%)
6 (R^1=3-Cl, R^2=H, method b, 33%)
7 (R^1=4-Cl, R^2=H, method a , 62%)
8 (R^1=2-Br, R^2=H, method b, 36%)
9 (R^1=3-Br, R^2=H, method b, 58%)
10 (R^1=4-Br, R^2=H, method b, 61%)
11 (R^1=2-OMe, R^2=H, method b, 41%)
12 (R^1=3-OMe, R^2=H, method b, 91%)
13 (R^1=4-OMe, R^2=H, method b, 73%)
14 (R^1=2-Me, R^2=H, method b , 27%)
15 (R^1=3-Me, R^2=H, method b, 45%)
16 (R^1=4-Me, , R^2=H, method b, 49%)
17 (R^1=2-CF_3, R^2=H, method b , 65%)
18 (R^1=3-CF_3, R^2=H, method b, 50%)
19 (R^1=4-CF_3, R^2=H, method b, 75%)
20 (R^1=2-Me, R^2=6-Me, method b, 24%)
21 (R^1=3-Me, R^2=5-Me, method b, 18%)
22 (R^1=2-Me, R^2=3-Me, method b, 28%)
23 (R^1=3-Me, R^2=4-Me, method b, 27%)
24 (R^1=2-Me, R^2=3-Cl, method b, 55%)
25 (R^1=3-Me, R^2=4-Cl, method b, 31%)
26 (R^1=4-Me, R^2=3-Cl, method b, 24%)

Figure 3. Structure of the carbamates investigated in this study.

4. Biological work

4.1. Inhibition of cell proliferation

The ability of compounds **1**-**26** to inhibit cell proliferation was established by means of their IC_{50} values towards the human tumor cell lines HT-29 (colon adenocarcinoma), MCF-7 (breast adenocarcinoma), HeLa (epithelioid cervix carcinoma), HL-60 (promyelocytic leukemia), A-549 (pulmonary adenocarcinoma) and MDA-MB-231 (breast adenocarcinoma) as well as towards the endothelial cell line HMEC-1 (human microvascular endothelial cells) and the non-tumor cell line HEK-293 (human embryonic kidney cells). The IC_{50} values are presented in Table 1 (nM) along with IC_{50} values for the parent compounds CA-4 and AmCA-4 (see Supporting Information for MDA-MB-231 cells).

Some trends can be deduced from Table 1. Thus, the majority of the compounds show activity in the low nanomolar range in all cell lines except in A549, in which the activity lies in the high nanomolar range. In general, carbamate derivatives show better IC_{50} values than AmCA-4 in most of the tested tumor cell lines. Moreover, halo- and methoxy-phenyl carbamates substituted at position 3 of the phenyl ring showed higher antiproliferative activity than their regioisomeric counterparts, particularly in MCF-7, HT-29, HeLa and A549 cell lines. As regards therapeutic range, compounds **4**, **5**, **6**, **9**, **10** and **19** show greater selectivity since the most of their IC_{50} values in MCF-7, HT-29, HeLa and HL-60 tumor cell lines are 2- to 11-fold lower than their IC_{50} values in the non-tumor cell line HEK-293. As regards endothelial cells (HMEC-1), compounds **6**, **10**, **12**, **25** and **26** show better antiproliferative activity than AmCA-4 (see table 1). These latter compounds are mainly substituted in *meta* and *para* positions with halogen atoms or their bioisosters.

Table 1. IC_{50} values (nM) for CA-4, AmCA-4 and derivatives **1**-**26**.[a]

Comp.	HT-29	MCF-7	HeLa	A549	HL-60	HMEC-1	HEK-293
CA-4	4200 ± 500	1000 ± 200	2100 ± 600	130 ± 20	4000 ± 1000	3400 ± 400	25000 ± 300

AmCA-4	22.0 ± 0.7	8.0 ± 0.9	2.6 ± 0.5	117 ± 7	4.5 ± 0.9	12 ± 6	7.1 ± 1.0
1	2.9 ± 0.5	9.8 ± 0.1	4.8 ± 0.2	77 ± 12	4 ± 2	12 ± 5	3.3 ± 0.2
2	110 ± 30	62 ± 2	17 ± 2	320 ± 190	4 ± 2	180 ± 20	65 ± 4
3	10.6 ± 0.5	7.0 ± 0.6	2.7 ± 1.3	150 ± 40	60 ± 20	20 ± 2	13.2 ± 0.2
4	60 ± 20	95.4 ± 1.3	60 ± 20	400 ± 200	50 ± 30	65 ± 13	185 ± 2
5	17.8 ± 0.7	10.1 ± 0.8	5 ± 2	130 ± 40	3.7 ± 0.7	50 ± 30	41 ± 2
6	9.2 ± 1.3	4.4 ± 0.6	4.79 ± 0.03	100 ± 20	13.5 ± 1.6	9 ± 6	14.5 ± 0.4
7	31 ± 14	82 ± 13	24 ± 3	800 ± 200	770 ± 170	76 ± 13	142 ± 9
8	7.5 ± 0.6	18.9 ± 0.9	2.6±1.0	180 ± 50	3 ± 2	22 ± 7	8 ± 5
9	11.3 ± 0.7	5.9 ± 0.3	2.6±0.5	160 ± 30	5.6 ± 0.6	12 ± 4	16 ± 2
10	3.5 ± 0.2	0.75 ± 0.05	1.2±0.2	150 ± 30	5 ± 3	7 ± 4	19 ± 7
11	290 ± 100	230 ± 180	348 ± 13	3000 ± 1100	350 ± 190	400 ± 15	160 ± 40
12	4.8 ± 0.5	7.18 ± 0.07	3.4 ± 0.4	160 ± 40	4.9 ± 0.5	5 ± 2	8.1 ± 0.2
13	350 ± 20	230 ± 30	200 ± 40	550 ± 120	50 ± 6	120 ± 50	130 ± 40
14	160 ± 70	380 ± 50	50 ± 30	460 ± 110	222 ± 7	55 ± 6	60 ± 20
15	46 ± 3	25 ± 9	23 ± 13	390 ± 180	67 ± 2	50 ± 20	40 ± 20
16	270 ± 80	200 ± 60	370 ± 160	1500 ± 300	52 ± 2	160 ± 40	144 ± 10
17	16 ± 7	44 ± 2	15 ± 4	110 ± 40	6.7 ± 0.6	19 ± 5	4.1 ± 1.0
18	13 ± 3	56 ± 9	40 ± 8	130 ± 60	4 ± 2	16 ± 5	42.2 ± 0.9
19	27.6 ± 0.6	9.2 ± 0.3	21 ± 8	270 ± 70	40 ± 30	30 ± 8	57 ± 22
20	600 ± 200	440 ± 14	320 ± 120	3900 ± 1200	470 ± 70	380 ± 140	490 ± 80
21	260 ± 140	210 ± 20	130 ± 16	1540 ± 80	620 ± 90	180 ± 7	150 ± 80
22	175 ± 4	16 ± 3	40 ± 20	900 ± 200	59 ± 13	140 ± 40	80 ± 30
23	130 ± 20	170 ± 30	21 ± 6	1300 ± 600	69 ± 11	130 ± 50	97 ± 9
24	47 ± 2	39 ± 3	23 ± 12	140 ± 30	70 ± 30	20 ± 2	14 ± 2
25	11.4 ± 0.3	8.1 ± 0.9	3.3 ± 0.5	140 ± 30	0.4 ± 0.2	7 ± 1	8.4 ± 0.6
26	23 ± 2	6.1 ± 0.8	3.7 ± 0.3	90 ± 20	1.8 ± 0.6	6 ± 2	7.0 ± 0.8

[a]IC_{50} values are expressed as the compound concentration (nM) that inhibits the cell growth by 50%. Data are the average (±SD) of three experiments.

4.2. Tubulin polymerization process

In order to evaluate the effects of the synthetic derivatives on tubulin self-assembly, the critical concentration (CrC) was determined. All compounds were tested at a concentration of 27.5 μM in glycerol-assembling buffer (GAB) and GTP to which tubulin was added at a concentration of 25 μM.

The results achieved with the carbamates are shown in table 2 and are compared with those attained in the absence of any ligand (control) and in the presence of CA-4 or AmCA-4.

Table 2. Critical Concentration (CrC) for the assembly of purified tubulin in GAB in the presence of CA-4, AmCA-4 or the carbamates.

Compound	CrC (μM)	Compound	CrC (μM)
Control	8 ± 1	**13**	23 ± 2
CA-4	22 ± 1	**14**	22 ± 3
AmCA-4	23 ± 2	**15**	20 ± 3
1	20 ± 2	**16**	25 ± 2
2	18 ± 3	**17**	23 ± 2
3	24 ± 4	**18**	14 ± 2
4	22 ± 2	**19**	20 ± 3
5	21 ± 3	**20**	17 ± 3
6	23 ± 2	**21**	24 ± 2
7	24 ± 2	**22**	25 ± 2
8	22 ± 2	**23**	21 ± 2
9	25 ± 3	**24**	23 ± 1
10	23 ± 2	**25**	24 ± 3
11	16 ± 1	**26**	24 ± 3
12	20 ± 2		

Data are the average (±SD) of three experiments.

All carbamates increased the CrC value relative to the value measured in the control (absence of ligand) with CrC values similar to those achieved in the presence of CA-4 or AmCA-4.

Figure 4 shows the effects of some selected ligands on the *in vitro* tubulin polymerization process studied by turbidimetry time-course measurements at 350 nm and at 37ºC. In order to compare, paclitaxel, a microtubule stabilizer, was also evaluated.

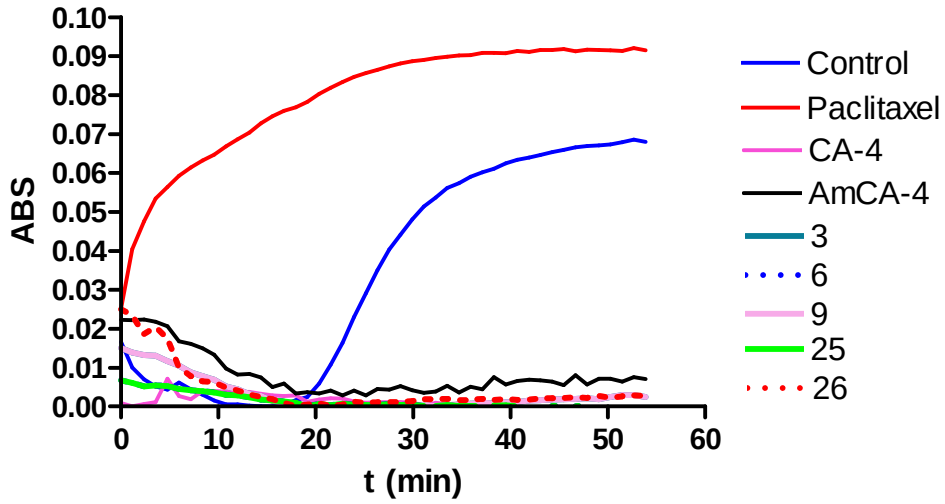

Figure 4. Effects of CA-4, AmCA-4 and carbamates on the in vitro tubulin polymerization.

4.3. Tubulin interaction at the colchicine binding site

In order to check whether the carbamates interact with tubulin in the colchicine-binding site the EBI assay was undertaken. This method is based on the property of *N*,*N*'-ethylene-bis(iodoacetamide) (EBI), a homobifunctional thioalkylating agent, to crosslink the Cys-239 and the Cys-354 residues present in the colchicine-binding site of β-tubulin. The covalent binding of EBI to β-tubulin forms an adduct that is easily detected by Western Blot as a second immunoreacting band of β-tubulin that migrates faster than the native β-tubulin band. As a consequence, treatment of the cells with a compound that binds to this colchicine-binding site will impair the binding of EBI, resulting in the absence of the second band [17]. The carbamates tested were selected according to their IC_{50} value in MDA-MB-231 (see Supporting Information), thus the three compounds with the lowest IC_{50} values (**10**, **12** and **25**) and two additional carbamates with higher IC_{50} values (**11** and **13**) were chosen for this study. With this selection we intended to ascertain if there was any correlation between the antiproliferative activity of the compounds and their capacity to interact with tubulin. The results of this assay are depicted in figure 5.

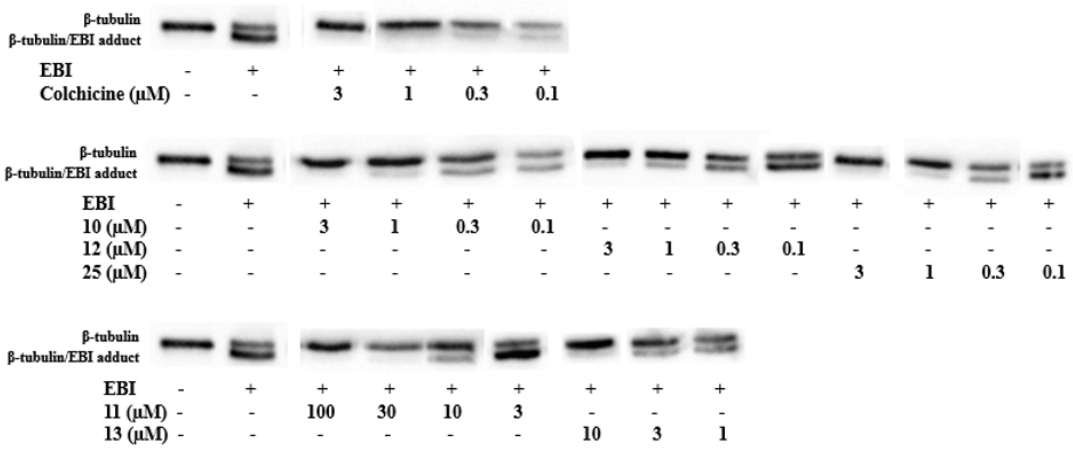

Figure 5. Effects of colchicine and carbamates at the colchicine-binding site of tubulin.

As shown in figure 5, there is a dose-response effect for all compounds tested. Concretely, compounds **10**, **12** and **25** were able to inhibit the formation of EBI adduct at 3 μM, showing a behaviour similar to that of colchicine at this concentration. However, compounds **11** and **13** were less effective since they required higher concentrations (100 μM for **11** and 10 μM for **13**) to avoid being displaced by EBI from tubulin. Thus, this experiment demonstrates that the compounds bind tubulin at the colchicine-binding site and that their antiproliferative capacity correlates with tubulin binding.

4.4. Mitotic arrest and inhibition of interphase microtubules of cultured

The effects of carbamates on cell cycle distribution were evaluated in A549 cells. Thus, cells were incubated for 20 h in the presence of CA-4, AmCA-4 and compounds **1**-**26** and then, DNA content was measured by flow cytometry (see experimental section). All the carbamates extensively arrested cells in the G2/M phase at a concentration half of their IC_{50} value.

Table 3. Cell cycle distribution (%).

Comp.	Conc (nM)	SubG0	G0/G1	S	G2/M
Control	-	6.6 ± 0.1	66 ± 1	16 ± 1	11 ± 1
CA-4	50	15 ± 1	21 ± 2	22 ± 1	43 ± 1
AmCA-4	60	14 ± 1	21 ± 1	24 ± 1	41 ± 2
1	40	20 ± 3	21 ± 1	15 ± 1	44 ± 3
2	160	17 ± 1	31 ± 3	13 ± 1	39 ± 2
3	75	19 ± 1	29 ± 1	10 ± 1	43 ± 2
4	200	21 ± 1	26 ± 5	19 ± 1	34 ± 1
5	65	16 ± 1	29 ± 2	12 ± 2	43 ± 3
6	50	16 ± 2	30 ± 1	10 ± 1	44 ± 2
7	400	20 ± 1	21 ± 1	18 ± 1	41 ± 1
8	90	17 ± 2	29 ± 1	10 ± 1	44 ± 3
9	80	17 ± 3	30 ± 1	12 ± 1	39 ± 1
10	75	19 ± 1	32 ± 3	17 ± 1	33 ± 1
11	1500	17 ± 1	29 ± 4	12 ± 3	43 ± 1
12	80	17 ± 1	31 ± 1	16 ± 2	36 ± 3
13	275	14 ± 1	25 ± 1	14 ± 1	46 ± 2
14	230	16 ± 1	31 ± 2	13 ± 2	40 ± 1
15	200	22 ± 3	26 ± 2	16 ± 3	36 ± 1
16	750	27 ± 5	24 ± 1	16 ± 2	32 ± 3
17	55	20 ± 2	21 ± 2	15 ± 1	44 ± 5
18	65	16 ± 3	28 ± 1	15 ± 1	41 ± 1
19	135	26 ± 1	22 ± 1	14 ± 1	39 ± 2
20	2000	23 ± 2	25 ± 2	17 ± 1	35 ± 1
21	750	22 ± 3	24 ± 3	16 ± 1	38 ± 1
22	450	12 ± 1	24 ± 1	22 ± 3	42 ± 2
23	650	17 ± 1	24 ± 1	19 ± 1	41 ± 1
24	70	20 ± 1	24 ± 1	18 ± 2	39 ± 1
25	70	18 ± 1	24 ± 1	22 ± 9	36 ± 8
26	45	29 ± 4	21 ± 1	14 ± 1	36 ± 3

Data are the average (±SD) of three experiments.

Next, we studied the effects of compounds **1-26** on the microtubule cytoskeleton. Therefore, A549 cells were incubated for 16 h in the presence of AmCA-4 and compounds **1**-**26** at concentrations twice their IC_{50} value. Figure 6 depicts some selected results. It can be appreciated that in the presence of AmCA-4 and carbamates, tubulin appears agregated and nuclei are compressed and fragmented, which is characteristic of cells that have been disturbed during their division process.

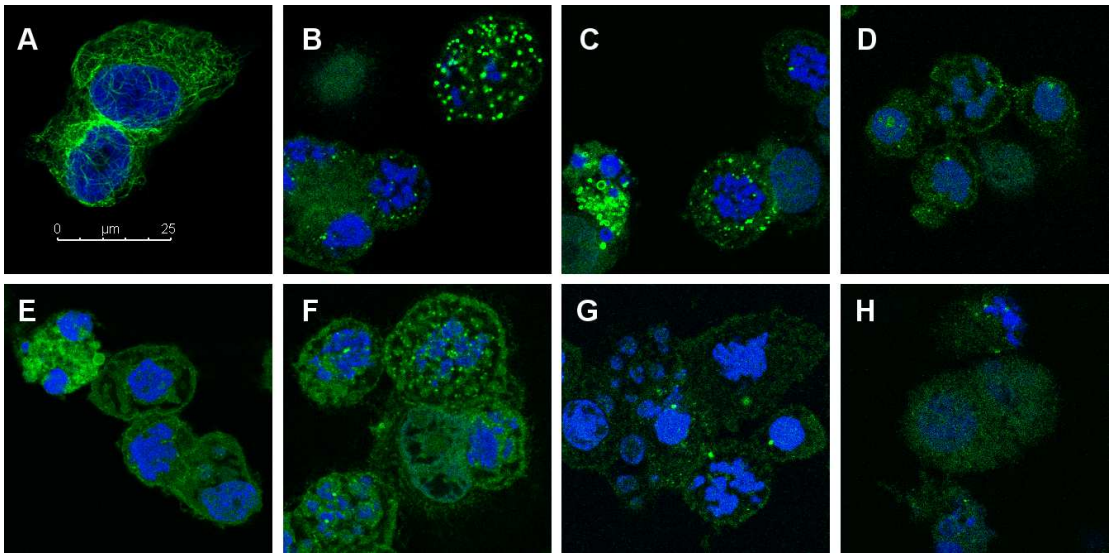

Figure 6. Effects of AmCA-4 and some selected carbamates on the microtubule network. A549 cells were treated for 16 hours and processed for immunofluorescence microscopy: (A) DMSO, (B) 230 nM AmCA-4, (C) 150 nM compound **1**, (D) 300 nM compound **3**, (E) 260 nM compound **5**, (F) 200 nM compound **6**, (G) 220 nM compound **17** and (H) 260 nM compound **18**.

4.5. Induction of apoptosis

Cell cycle distribution (Table 3) clearly shows that the percentage of subG0 cells is increased in cells treated with CA-4, AmCA-4 and carbamates. This exhibition of a sub-diploid DNA content, together with the high percentage of cells arrested in mitotic phase, could be characteristic of apoptosis. Consequently, induction of apoptosis was studied by measuring the translocation of phosphatidylserine from the cytoplasmic to the extracellular side of the plasma membrane. Thus, A549 cells were incubated for 20 h in the presence of AmCA-4 and some representative carbamates, after which

annexin content was measured by flow cytometry. Carbamates which displayed the best antiproliferative activity were selected for this assay.

From figure 7 it can be concluded that carbamates induce apoptosis at both concentrations tested. With exception of compound **26**, all of them are more active than AmCA-4 at 100 nM. Moreover, compounds **9** and **12** show a similar effect to AmCA-4 at 10 nM.

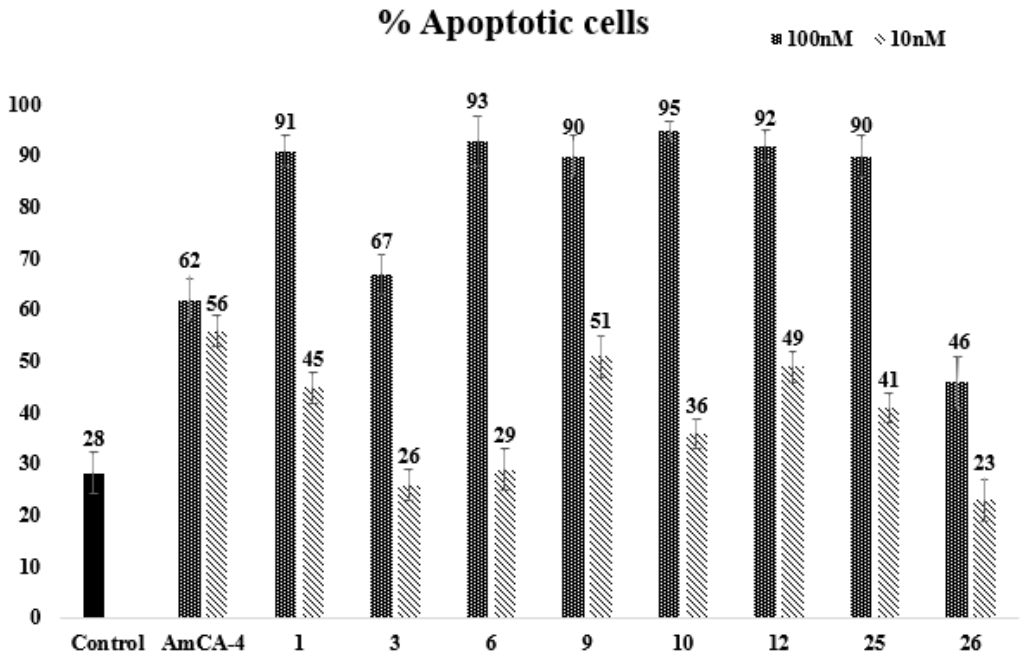

Figure 7. Apoptotic effect of AmCA-4 and carbamates. Data are the average (±SD) of three experiments.

4.6. Tube destruction

Vascular-disrupting agents do not only affect tumor cells but also endothelial cells. Thus, the capacity of synthetic carbamates to destroy a preexisting vasculature network formed by endothelial cells was evaluated. Therefore, cells were seeded on top of Matrigel, which induces the formation of a network of endothelial tubes. Then, the cultures were treated with different concentrations of AmCA-4 and carbamates and pictures were taken 4 h later in order to evaluate the tube destruction effect.

Carbamates with the best antiproliferative activity in HMEC-1 cells (compounds **10**, **12** and **25)** were selected for this assay. Additionally, two less active carbamates (**11** and **13**) were tested in order to establish a correlation between antiproliferative capacity and tube destruction. As shown in figure 8, all compounds tested displayed a vascular disrupting activity in a dose-dependent manner. Concretely, compounds **10**, **12** and **25** exhibited this property at concentrations higher than 3 nM, improving the effect manifested by AmCA-4 and being about 10-fold more active than **13** and 100-fold more active than **11**. Therefore, the higher the antiproliferative activity, the greater the capacity for tube destruction cycle distribution.

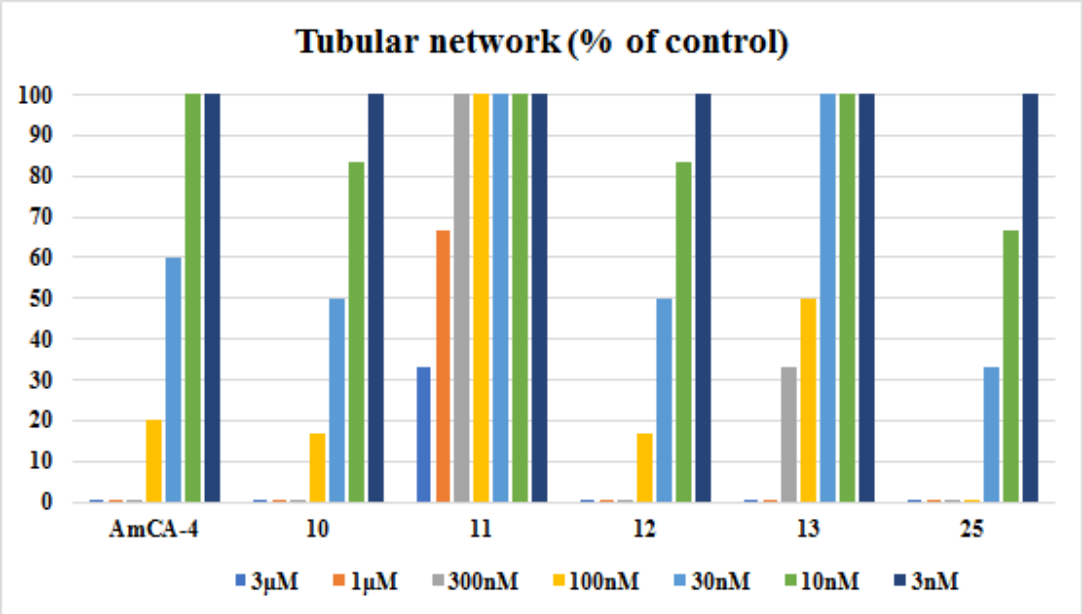

Figure 8. Tube destruction effect of selected carbamates. All the compounds were tested at 3 μM, 1 μM, 300 nM, 30 nM, 10 nM and 3 nM.

The images obtained for carbamate **25** are shown in figure 9. This compound was able to totally destroy the vascular network at 100 nM, whereas in the presence of 100 nM of AmCA-4 or compounds **10** and **12**, part of the vascular network remained intact.

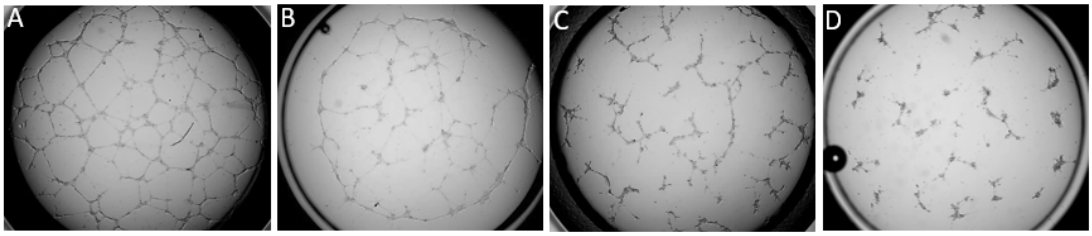

Figure 9. Effect of carbamate **25** on the tubular network. (A) 3 nM, (B) 10 nM, (C) 30 nM, (D) 100 nM.

4. Summary and conclusions

The effect of introduction of a carbamate group in the aminocombretastatin structure was studied. As shown in table 1, carbamate derivatives offer IC_{50} values in the nanomolar range, improving by far the activity of CA-4 and, in some cases, the activity of AmCA-4. For instance, derivatives **6** (*m*-Cl), **9** (*m*-Br), **10** (*p*-Br), **12** (*m*-OMe) exceeded the activity of AmCA-4 in HT-29, MCF-7 and HMEC-1 cell lines and also offered a good selectivity over non-tumor cell lines. From the structures of these compounds it can be concluded that the most active carbamates are the ones bearing chloro, bromo or methoxy groups in the *meta* position of the phenyl ring.

In addition, all the carbamates proved as potent as CA-4 and AmCA-4 in inhibiting *in vitro* tubulin polymerization. We also demonstrated that carbamates interact with tubulin at the colchicine-binding site and that the compounds with higher antiproliferative activity (compounds **10** (*p*-Br), **12** (*m*-OMe) and **25** (*m*-Me-*p*-Cl) also show greater tubulin binding capacity. From cell cycle analysis and immunofluorescence studies it can be deduced that carbamates cause a mitotic arrest in A549 cells causing nuclei fragmentation and tubulin aggregation. Moreover, the carbamates induced apoptosis in a dose-dependent manner, with more than 90% of apoptotic cells at 100 nM. Compounds **9** (*m*-Br) and **12** (*m*-OMe) proved as active as AmCA-4 even at a concentration of 10 nM.

Finally, some selected carbamates displayed a vascular disrupting activity of endothelial cells in a dose-dependent manner which correlated with their antiproliferative activity. Thus, highly anti-proliferative carbamates **10** (*p*-Br), **12** (*m*-OMe) and **25** (*m*-Me-*p*-Cl) were able to disrupt tubular network at concentrations higher than 3 nM, improving the effect shown by AmCA-4.

5. Experimental

5.1. Chemistry

5.1.1. General procedures

NMR spectra were measured at 25°C. The signals of the deuterated solvent ($CDCl_3$) were taken as the reference. Multiplicity assignments of ^{13}C signals were made by means of the DEPT pulse sequence. Complete signal assignments in ^{1}H and ^{13}C NMR spectra were made with the aid of 2D homo- and heteronuclear pulse sequences (COSY, HSQC, HMBC). High resolution mass spectra were run by the electrospray mode (ESMS). IR data were measured with oily films on NaCl plates (oils) and are given only for relevant functional groups (C=O, NH). Experiments which required an inert atmosphere were carried out under dry N_2 in flame-dried glassware. Commercially available reagents were used as received.

5.1.2. Experimental procedure for the synthesis of carbamates by method a.

A solution of AmCA-4 (0.7 mmol) in THF (5 mL/mmol) was cooled at 0ºC and anhydrous pyridine (1.7 mmol) and the corresponding phenyl chloroformate (1.0 mmol) were added under inert atmosphere. The resulting mixture was stirred in the dark for 20 min at 0ºC and for 1 h at rt. After this time, H_2O (3.4 mL) and HCl 1M (1.7 mL) were added to the reaction mixture, which was then extracted with CH_2Cl_2 (3 x 20 mL). The organic layer was washed with brine, and then dried on anhydrous Na_2SO_4. Removal of volatiles under reduced pressure afforded an oily residue which was

subjected to column chromatography on silica-gel (Hexanes-EtOAc mixtures as eluant) obtaining the desired products with the yields indicated below.

Phenyl *(Z)*-(2-methoxy-5-(3,4,5-trimethoxystyryl)phenyl)carbamate (1): off-white solid, m. p. 124-126ºC; ^{1}H NMR (500 MHz, $CDCl_3$) δ 8.11 (br s, 1H), 7.52 (br s, 1H, NH), 7.39 (t, *J* ~ 7.5 Hz, 2H), 7.24 (t, *J* ~ 7.5 Hz, 1H), 7.19 (d, ~ 7.5 Hz, 2H), 7.00 (d, *J* = 8.5 Hz, 1H), 6.76 (d, *J* = 8.5 Hz, 1H), 6.52 (s, 2H), 6.51 (d, *J* = 12 Hz, 1H), 6.45 (d, *J* = 12 Hz, 1H), 3.89 (s, 3H), 3.81 (s, 3H), 3.70 (s, 6H); ^{13}C NMR (125 MHz, $CDCl_3$) δ (C) 152.9 (x 2), 151.3, 150.6, 146.9, 137.2, 132.7, 130.3, 126.9, (CH) 129.5, 129.3 (x 2), 129.2, 125.5, 123.9, 121.6 (x 2), 119.3, 109.6, 106.1 (x 2), (CH_3) 60.8, 55.9 (x 2), 55.8; IR ν_{max} (cm^{-1}) 3415 (N−H), 1750 (C=O); HR ESMS *m/z* 458.1588 $[M+Na]^+$. Calc. for $C_{25}H_{25}NNaO_6$, 458.1580.

4-Fluorophenyl *(Z)*-(2-methoxy-5-(3,4,5-trimethoxystyryl)phenyl)carbamate (4): yellowish solid, m. p. 138-142ºC; ^{1}H NMR (500 MHz, $CDCl_3$) δ 8.10 (s, 1H), 7.50 (s, 1H), 7.14 (dd, *J* = 9, 4.5 Hz, 2H), 7.07 (t, *J* ~ 9 Hz, 2H), 7.01 (dd, *J* = 8.5, 2 Hz, 1H), 6.76 (d, *J* = 8.5 Hz, 1H), 6.52 (s, 2H), 6.50 (d, *J* = 12 Hz, 1H), 6.45 (d, *J* = 12 Hz, 1H), 3.90 (s, 3H), 3.82 (s, 3H), 3.70 (s, 6H); ^{13}C NMR (125 MHz, $CDCl_3$) δ (C) 160.1 (center point of doublet with $^{1}J_{C-F}$ ~ 242 Hz), 152.9 (x 2), 146.9, 146.5, 146.4, 137.2, 132.7, 130.3, 126.7, (CH) 129.5, 129.3, 124.1, 123.1 (x 2, doublet with $^{3}J_{C-F}$ ~ 7.5 Hz), 119.3*, 115.9 (x 2, doublet with $^{2}J_{C-F}$ ~ 23 Hz), 109.7, 106.1 (x 2), (CH_3) 60.8, 55.9 (x 2), 55.8 (starred signal is low and broad); IR ν_{max} (cm^{-1}) 3416 (N−H), 1747 (C=O); HR ESMS *m/z* 476.1484 $[M+Na]^+$. Calc. for $C_{25}H_{24}FNNaO_6$, 476.1485.

4-Chlorophenyl *(Z)*-(2-methoxy-5-(3,4,5-trimethoxystyryl)phenyl)carbamate (7): off-white solid, m. p. 138-140ºC; ^{1}H NMR (500 MHz, $CDCl_3$) δ 8.06 (br s, 1H), 7.50 (br s, 1H, NH), 7.35 (apparent d, *J* = 8.8 Hz, 2H), 7.13 (apparent d, *J* = 8.8 Hz, 2H), 7.01 (dd, *J* = 8.5, 2.5 Hz, 1H), 6.76 (d, *J* = 8.5 Hz, 1H),

6.51 (s, 2H), 6.50 (d, *J* = 12 Hz, 1H), 6.46 (d, *J* = 12 Hz, 1H), 3.89 (s, 3H), 3.81 (s, 3H), 3.70 (s, 6H); ^{13}C NMR (125 MHz, $CDCl_3$) δ (C) 152.8 (x 2), 150.9, 149.1, 146.9, 137.2, 132.6, 130.8, 130.3, 126.6, (CH) 129.4, 129.3 (x 2), 124.1, 122.9 (x 2), 119.3*, 109.7, 106.1 (x 2), (CH_3) 60.7, 55.8, 55.8 (x 2) (starred signal is low and broad); IR ν_{max} (cm^{-1}) 3414 (N-H), 1749 (C=O); HR ESMS *m/z* 492.1189 $[M+Na]^+$. Calc. for $C_{25}H_{24}{}^{35}ClNNaO_6$, 492.1190.

5.1.3. Experimental procedure for the synthesis of carbamates by method b.

A solution of AmCA-4 (0.14 mmol) in THF (4 mL/mmol) was added to a solution of triphosgene (0.3 mmol) in THF (0.7 ml/mmol). The resulting mixture was stirred in the dark for 10 min at rt. Then Et_3N (4.3 mmol) was slowly added and the resulting residue was resuspended in THF (0.8 mL). The corresponding phenol (0.8 mmol) was added to the mixture which was stirred in the dark for 1 h at 45ºC. After this time, volatiles were removed under reduced pressure and the remaining residue was dissolved in acetone. The precipitated which remained without dissolving was discarded by simple filtration, and then the filtrate was concentrated under reduced pressure to give an oily residue which was subjected to column chromatography on silica-gel (Hexanes-EtOAc mixtures as eluant) affording the desired products with the yields indicated below.

2-Fluorophenyl *(Z)*-(2-methoxy-5-(3,4,5-trimethoxystyryl)phenyl)carbamate (2): yellowish solid, m. p. 138-142ºC; ^{1}H NMR (500 MHz, $CDCl_3$) δ 8.10 (s, 1H), 7.60 (s, 1H), 7.30-7.15 (br m, 4H), 7.00 (dd, *J* = 8.5, 2 Hz, 1H), 6.76 (d, *J* = 8.5 Hz, 1H), 6.52 (s, 2H), 6.50 (d, *J* = 12 Hz, 1H), 6.45 (d, *J* = 12 Hz, 1H), 3.90 (s, 3H), 3.78 (s, 3H), 3.70 (s, 6H); ^{13}C NMR (125 MHz, $CDCl_3$) δ (C) 154.6 (center point of doublet with $^1J_{C-F}$ ~ 248 Hz), 152.9 (x 2), 150.2*, 146.9, 138.0 (doublet with $^2J_{C-F}$ ~ 11.5 Hz), 137.2, 132.7, 130.3, 126.6, (CH) 129.5, 129.3, 126.8 (doublet with $^3J_{C-F}$ ~ 7.5 Hz), 124.3 (doublet with $^3J_{C-F}$ ~ 3.8 Hz), 124.2, 124.1, 119.2*, 116.6 (doublet with $^2J_{C-F}$ ~ 18.5 Hz), 109.7, 106.1 (x 2), (CH_3) 60.8,

55.9 (x 2), 55.8 (starred signals are low and broad); IR ν_{max} (cm^{-1}) 3416 (N−H), 1753 (C=O); HR ESMS *m/z* 476.1484 $[M+Na]^+$. Calc. for $C_{25}H_{24}FNNaO_6$, 476.1485.

3-Fluorophenyl *(Z)*-(2-methoxy-5-(3,4,5-trimethoxystyryl)phenyl)carbamate (3): off-white solid, m. p. 127-130ºC; ^1H NMR (500 MHz, $CDCl_3$) δ 8.07 (br s, 1H), 7.50 (br s, 1H, NH), 7.34 (apparent q, *J* ~ 7.7 Hz, 1H), 7.02 (dd, *J* = 8.5, 1.5 Hz, 1H), 7.00-6.95 (m, 3H), 6.76 (d, *J* = 8.5 Hz, 1H), 6.52 (s, 2H), 6.51 (d, *J* = 12 Hz, 1H), 6.46 (d, *J* = 12 Hz, 1H), 3.90 (s, 3H), 3.81 (s, 3H), 3.70 (s, 6H); ^{13}C NMR (125 MHz, $CDCl_3$) δ (C) 162.8 (center point of doublet with $^1J_{C–F}$ ~ 246 Hz), 152.9 (x 2), 151.5 (doublet with $^3J_{C–F}$ ~ 10 Hz), 150.7*, 146.9, 137.2, 132.7, 130.4, 126.6, (CH) 130.0 (doublet with $^3J_{C–F}$ ~ 8.5 Hz), 129.5, 129.4, 124.2, 119.3*, 117.3 (doublet with $^4J_{C–F}$ ~ 3 Hz), 112.5 (doublet with $^2J_{C–F}$ ~ 10 Hz), 109.7 (doublet with $^2J_{C–F}$ ~ 5 Hz), 109.6, 106.1 (x 2), (CH_3) 60.8, 55.9 (x 2), 55.8 (starred signals are low and broad); IR ν_{max} (cm^{-1}) 3413 (N−H), 1753 (C=O); HR ESMS *m/z* 476.1482 $[M+Na]^+$. Calc. for $C_{25}H_{24}FNNaO_6$, 476.1485.

2-Chlorophenyl *(Z)*-(2-methoxy-5-(3,4,5-trimethoxystyryl)phenyl)carbamate (5): off-white solid, m. p. 130-131ºC; ^1H NMR (500 MHz, $CDCl_3$) δ 8.11 (br s, 1H), 7.65 (br s, 1H, NH), 7.45 (dd, *J* = 7.8, 1.5 Hz, 1H), 7.30-7.20 (m, 3H), 7.01 (dd, *J* = 8.5, 2 Hz, 1H), 6.76 (d, *J* = 8.5 Hz, 1H), 6.52 (s, 2H), 6.49 (d, *J* = 12 Hz, 1H), 6.44 (d, *J* = 12 Hz, 1H), 3.90 (s, 3H), 3.78 (s, 3H), 3.70 (s, 6H); ^{13}C NMR (125 MHz, $CDCl_3$) δ (C) 152.9 (x 2), 146.9, 146.7, 137.2, 132.7, 130.3, 130.0, 127.4, 126.7, (CH) 130.3, 129.5, 129.3, 127.6, 126.9, 124.2, 124.1, 119.2*, 109.7, 106.1 (x 2), (CH_3) 60.8, 55.9 (x 2) (starred signal is low and broad), 55.8; IR ν_{max} (cm^{-1}) 3413 (N−H), 1755 (C=O); HR ESMS *m/z* 492.1188 $[M+Na]^+$. Calc. for $C_{25}H_{24}{}^{35}ClNNaO_6$, 492.1190.

3-Chlorophenyl *(Z)*-(2-methoxy-5-(3,4,5-trimethoxystyryl)phenyl)carbamate (6): off-white solid, m. p. 128-130ºC; ^1H NMR (500 MHz, $CDCl_3$) δ 8.07 (br s, 1H), 7.50 (br s, 1H, NH), 7.31 (t, *J* = 8.3 Hz,

1H), 7.22 (m, 2H), 7.09 (dd, *J* = 8.3, 1.5 Hz, 1H), 7.01 (dd, *J* = 8.5, 2 Hz, 1H), 6.76 (d, *J* = 8.5 Hz, 1H), 6.52 (s, 2H), 6.51 (d, *J* = 12 Hz, 1H), 6.46 (d, *J* = 12 Hz, 1H), 3.89 (s, 3H), 3.81 (s, 3H), 3.70 (s, 6H); ^{13}C NMR (125 MHz, $CDCl_3$) δ (C) 152.9 (x 2), 151.1, 150.7*, 146.9*, 137.2, 134.5, 132.7, 130.3, 126.5, (CH) 130.0, 129.5, 129.4, 125.8, 124.2, 122.2, 119.9*, 119.3, 109.7, 106.1 (x 2), (CH_3) 60.8, 55.9 (x 2), 55.8 (starred signals are low and broad); IR ν_{max} (cm^{-1}) 3413 (N−H), 1754 (C=O); HR ESMS *m/z* 492.1189 $[M+Na]^+$. Calc. for $C_{25}H_{24}{}^{35}ClNNaO_6$, 492.1190.

2-Bromophenyl *(Z)*-(2-methoxy-5-(3,4,5-trimethoxystyryl)phenyl)carbamate (8): off-white solid, m. p. 130-132ºC; ^{1}H NMR (500 MHz, $CDCl_3$) δ 8.11 (br s, 1H), 7.60 (br s, 1H, NH), 7.61 (dd, *J* = 7.8, 1.5 Hz, 1H), 7.34 (td, *J* = 7.8, 1.5 Hz, 1H), 7.24 (dd, *J* = 7.8, 1.5 Hz, 1H), 7.13 (td, *J* = 7.8, 1.5 Hz, 1H), 7.01 (dd, *J* = 8.5, 2 Hz, 1H), 6.76 (d, *J* = 8.5 Hz, 1H), 6.52 (s, 2H), 6.49 (d, *J* = 12 Hz, 1H), 6.45 (d, *J* = 12 Hz, 1H), 3.90 (s, 3H), 3.78 (s, 3H), 3.70 (s, 6H); ^{13}C NMR (125 MHz, $CDCl_3$) δ (C) 152.9 (x 2), 150.2*, 147.9, 146.9*, 137.2, 132.7, 130.3, 126.6, 116.6, (CH) 133.2, 129.4, 129.2, 128.3, 127.2, 124.2, 124.1, 119.2*, 109.7, 106.1 (x 2), (CH_3) 60.8, 55.9 (x 2), 55.8 (starred signals are low and broad); IR ν_{max} (cm^{-1}) 3413 (N−H), 1754 (C=O); HR ESMS *m/z* 536.0685 $[M+Na]^+$. Calc. for $C_{25}H_{24}{}^{79}BrNNaO_6$, 536.0685.

3-Bromophenyl *(Z)*-(2-methoxy-5-(3,4,5-trimethoxystyryl)phenyl)carbamate (9): off-white solid, m. p. 102-105ºC; ^{1}H NMR (500 MHz, $CDCl_3$) δ 8.07 (br s, 1H), 7.50 (br s, 1H, NH), 7.40-7.35 (m, 2H), 7.25 (t, *J* = 8 Hz, 1H), 7.14 (br d, *J* ~ 8 Hz, 1H), 7.01 (dd, *J* = 8.5, 2 Hz, 1H), 6.76 (d, *J* = 8.5 Hz, 1H), 6.51 (s, 2H), 6.50 (d, *J* = 12 Hz, 1H), 6.46 (d, *J* = 12 Hz, 1H), 3.89 (s, 3H), 3.81 (s, 3H), 3.70 (s, 6H); ^{13}C NMR (125 MHz) δ (C) 152.9 (x 2), 151.1, 150.7*, 146.9*, 137.2, 132.7, 130.3, 126.5, 122.2, (CH) 130.3, 129.4, 129.3, 128.7, 125.1, 124.2*, 120.4, 119.3*, 109.7, 106.1 (x 2), (CH_3) 60.8, 55.9 (x 2), 55.8 (starred signals are low and broad); IR ν_{max} (cm^{-1}) 3412 (N−H), 1753 (C=O); HR ESMS *m/z* 536.0687 $[M+Na]^+$. Calc. for $C_{25}H_{24}{}^{79}BrNNaO_6$, 536.0685.

4-Bromophenyl *(Z)*-(2-methoxy-5-(3,4,5-trimethoxystyryl)phenyl)carbamate (10): off-white solid, m. p. 146-149ºC; ^{1}H NMR (500 MHz, $CDCl_3$) δ 8.06 (br s, 1H), 7.50 (br s, 1H, NH), 7.48 (apparent d, *J* = 8.8 Hz, 2H), 7.07 (apparent d, *J* = 8.8 Hz, 2H), 7.01 (dd, *J* = 8.5, 2.0 Hz, 1H), 6.76 (d, *J* = 8.5 Hz, 1H), 6.51 (s, 2H), 6.50 (d, *J* = 12 Hz, 1H), 6.45 (d, *J* = 12 Hz, 1H), 3.89 (s, 3H), 3.81 (s, 3H), 3.70 (s, 6H); ^{13}C NMR (125 MHz) δ (C) 152.9 (x 2), 150.8*, 149.7, 146.9, 137.2, 132.7, 130.3, 126.6, 118.5, (CH) 132.3 (x 2), 129.4, 129.3, 124.1, 123.3 (x 2), 119.3*, 109.7, 106.1 (x 2), (CH_3) 60.8, 55.9 (x 2), 55.8 (starred signals are low and broad); IR ν_{max} (cm^{-1}) 3415 (N−H), 1749 (C=O); HR ESMS *m/z* 536.0690 $[M+Na]^+$. Calc. for $C_{25}H_{24}{}^{79}BrNNaO_6$, 536.0685.

2-Methoxyphenyl (*Z*)-(2-methoxy-5-(3,4,5-trimethoxystyryl)phenyl)carbamate (11): off-white solid, m. p. 110-113ºC; ^{1}H NMR (500 MHz, $CDCl_3$) δ 8.13 (br s, 1H), 7.60 (br s, 1H, NH), 7.22 (td, *J* = 8.3, 2 Hz, 1H), 7.14 (dd, *J* = 7.8, 1.5 Hz, 1H), 7.00-6.95 (br m, 3H), 6.75 (d, *J* = 8.5 Hz, 1H), 6.52 (s, 2H), 6.50 (d, *J* = 12 Hz, 1H), 6.43 (d, *J* = 12 Hz, 1H), 3.89 (s, 3H), 3.86 (s, 3H), 3.79 (s, 3H), 3.70 (s, 6H); ^{13}C NMR (125 MHz) δ (C) 152.8 (x 2), 151.7, 151.0, 146.8, 139.5, 137.2, 132.7, 130.3, 127.1, (CH) 129.6, 129.1, 126.7, 123.7, 123.3, 120.7, 119.1*, 112.4, 109.6, 106.1 (x 2), (CH_3) 60.8, 55.9 (x 3), 55.8; IR ν_{max} (cm^{-1}) 3413 (N−H), 1751 (C=O); HR ESMS *m/z* 488.1684 $[M+Na]^+$. Calc. for $C_{26}H_{27}NNaO_7$, 488.1685.

3-Methoxyphenyl (*Z*)-(2-methoxy-5-(3,4,5-trimethoxystyryl)phenyl)carbamate (12): off-white solid, m. p. 105-108ºC; ^{1}H NMR (500 MHz, $CDCl_3$) δ 8.10 (br s, 1H), 7.50 (br s, 1H, NH), 7.28 (t, *J* = 8 Hz, 1H), 7.00 (dd, *J* = 8.3, 2 Hz, 1H), 6.79 (dt, *J* = 8, 2 Hz, 2H), 6.75 (m, 2H), 6.52 (s, 2H), 6.51 (d, *J* = 12 Hz, 1H), 6.45 (d, *J* = 12 Hz, 1H), 3.88 (s, 3H), 3.80 (s, 6H), 3.69 (s, 6H); ^{13}C NMR (C) 160.4, 152.9 (x 2), 151.6*, 151.2*, 146.9, 137.2, 132.7, 130.3, 126.8, (CH) 129.6, 129.5, 129.2, 123.9, 119.3*, 113.8, 111.5, 109.6, 107.6, 106.1 (x 2), (CH_3) 60.8, 55.9 (x 2), 55.8, 55.3 (starred signals are low and broad);

IR ν_{max} (cm^{-1}) 3421 (N−H), 1751 (C=O); HR ESMS *m/z* 488.1683 $[M+Na]^+$. Calc. for $C_{26}H_{27}NNaO_7$, 488.1685.

4-Methoxyphenyl (*Z*)-(2-methoxy-5-(3,4,5-trimethoxystyryl)phenyl)carbamate (13): off-white solid, m. p. 136-138ºC; ^{1}H NMR (500 MHz, $CDCl_3$) δ 8.10 (br s, 1H), 7.50 (br s, 1H, NH), 7.09 (apparent d, *J* ~ 9 Hz, 2H), 6.99 (dd, *J* = 8.5, 2 Hz, 1H), 6.89 (apparent d, *J* ~ 9 Hz, 2H), 6.75 (d, *J* = 8.5 Hz, 1H), 6.52 (s, 2H), 6.50 (d, *J* = 12 Hz, 1H), 6.44 (d, *J* = 12 Hz, 1H), 3.88 (s, 3H), 3.81 (s, 3H), 3.80 (s, 3H), 3.70 (s, 6H); ^{13}C NMR (C) 157.1, 152.8 (x 2), 151.8*, 146.8, 144.1, 137.2, 132.7, 130.3, 126.9, (CH) 129.5, 129.2, 123.8, 122.4 (x 2), 119.2*, 114.3 (x 2), 109.6, 106.1 (x 2), (CH_3) 60.8, 55.8 (x 3), 55.5 (starred signals are low and broad); IR ν_{max} (cm^{-1}) 3419 (N−H), 1748 (C=O); HR ESMS *m/z* 488.1686 $[M+Na]^+$. Calc. for $C_{26}H_{27}NNaO_7$, 488.1685.

***o*-Tolyl (*Z*)-(2-methoxy-5-(3,4,5-trimethoxystyryl)phenyl)carbamate (14):** off-white solid, m. p. 146-148ºC; ^{1}H NMR (500 MHz, $CDCl_3$) δ 8.12 (br s, 1H), 7.55 (br s, 1H, NH), 7.25-7.20 (m, 2H), 7.16 (apparent t, *J* ≈ 7.5 Hz, 1H), 7.10 (d, *J* = 7.5 Hz, 1H), 7.01 (dd, *J* = 8.5, 1.5 Hz, 1H), 6.76 (d, *J* = 8.5 Hz, 1H), 6.52 (s, 2H), 6.50 (d, *J* = 12 Hz, 1H), 6.44 (d, *J* = 12 Hz, 1H), 3.91 (s, 3H), 3.79 (s, 3H), 3.70 (s, 6H), 2.27 (s, 3H); ^{13}C NMR (C) 152.9 (x 2), 151.2*, 149.1, 146.8, 137.2, 132.7, 130.7, 130.3, 127.0, (CH) 131.1, 129.6, 129.2, 126.8, 125.9, 123.9, 122.2, 119.2*, 109.6, 106.1 (x 2), (CH_3) 60.8, 55.9 (x 2), 55.8, 16.1 (starred signals are low and broad); IR ν_{max} (cm^{-1}) 3424 (N−H), 1750 (C=O); HR ESMS *m/z* 472.1727 $[M+Na]^+$. Calc. for $C_{26}H_{27}NNaO_6$, 472.1736.

***m*-Tolyl (*Z*)-(2-methoxy-5-(3,4,5-trimethoxystyryl)phenyl)carbamate (15):** yellowish solid, m. p. 113-115ºC; ^{1}H NMR (500 MHz, $CDCl_3$) δ 8.10 (br s, 1H), 7.50 (br s, 1H, NH), 7.28 (apparent t, *J* ≈ 7.5 Hz, 1H), 7.10-7.00 (m, 4H), 6.76 (d, *J* = 8.5 Hz, 1H), 6.52 (s, 2H), 6.51 (d, *J* ≈ 12 Hz, 1H), 6.45 (d, *J* = 12 Hz, 1H), 3.90 (s, 3H), 3.81 (s, 3H), 3.71 (s, 6H), 2.38 (s, 3H); ^{13}C NMR (C) 152.8 (x 2), 151.5*, 150.5, 146.8*, 139.4, 137.2, 132.7, 130.3, 126.9, (CH) 129.5, 129.2, 129.0, 126.3, 123.8, 122.2, 119.3*,

118.5, 109.6, 106.1 (x 2), (CH_3) 60.8, 55.9 (x 2), 55.8, 21.2 (starred signals are low and broad); IR ν_{max} (cm^{-1}) 3426 (N−H), 1750 (C=O); HR ESMS *m/z* 472.1738 $[M+Na]^+$. Calc. for $C_{26}H_{27}NNaO_6$, 472.1736.

***p*-Tolyl (*Z*)-(2-methoxy-5-(3,4,5-trimethoxystyryl)phenyl)carbamate (16):** off-white solid, m. p. 162-164ºC; ^{1}H NMR (500 MHz, $CDCl_3$) δ 8.10 (br s, 1H), 7.50 (br s, 1H, NH), 7.18 (apparent d, *J* = 8 Hz, 2H), 7.06 (apparent d, *J* = 8, Hz, 2H), 7.00 (dd, *J* = 8.5, 2 Hz, 1H), 6.75 (d, *J* = 8.5 Hz, 1H), 6.52 (s, 2H), 6.50 (d, *J* = 12 Hz, 1H), 6.44 (d, *J* = 12 Hz, 1H), 3.89 (s, 3H), 3.81 (s, 3H), 3.70 (s, 6H), 2.36 (s, 3H); ^{13}C NMR (C) 152.9 (x 2), 151.6*, 148.4, 146.9, 137.2, 135.2, 132.7, 130.3, 127.0, (CH) 129.8 (x 2), 129.6, 129.2, 123.8, 121.3 (x 2), 119.3*, 109.6, 106.1 (x 2), (CH_3) 60.8, 55.9 (x 2), 55.8, 20.8 (starred signals are low and broad); IR ν_{max} (cm^{-1}) 3425 (N−H), 1750 (C=O); HR ESMS *m/z* 472.1728 $[M+Na]^+$. Calc. for $C_{26}H_{27}NNaO_6$, 472.1736.

2-(Trifluoromethyl)phenyl (*Z*)-(2-methoxy-5-(3,4,5-trimethoxystyryl)phenyl)carbamate (17): off-white solid, m. p. 132-134ºC; ^{1}H NMR (500 MHz, $CDCl_3$) δ 8.09 (br s, 1H), 7.68 (d, *J* = 7.8 Hz, 1H), 7.60-7.55 (m, 2H), 7.35 (m, 2H), 7.01 (d, *J* = 8.5 Hz, 1H), 6.77 (d, *J* = 8.5 Hz, 1H), 6.52 (s, 2H), 6.50 (d, *J* = 12 Hz, 1H), 6.45 (d, *J* = 12 Hz, 1H), 3.90 (s, 3H), 3.77 (s, 3H), 3.70 (s, 6H); ^{13}C NMR (C) 152.9 (x 2), 150.4*, 148.0, 147.0, 137.2, 130.3, 126.5, 123.1 (quadruplet with $^2J_{C-F}$ ~ 31 Hz), 121.9, (CH) 132.8, 129.4, 129.3, 126.8 (quadruplet with $^3J_{C-F}$ ~ 4 Hz), 125.7, 124.6, 124.3, 119.2*, 109.7, 106.0 (x 2), (CH_3) 60.8, 55.9 (x 3) (starred signals are low and broad). IR ν_{max} (cm^{-1}) 3425 (N−H), 1762 (C=O); HR ESMS *m/z* 526.1448 $[M+Na]^+$. Calc. for $C_{26}H_{24}F_3NNaO_6$, 526.1453.

3-(Trifluoromethyl)phenyl (*Z*)-(2-methoxy-5-(3,4,5-trimethoxystyryl)phenyl)carbamate (18): viscous oil; ^{1}H NMR (500 MHz, $CDCl_3$) δ 8.06 (br s, 1H), 7.55-7.45 (m, 4H), 7.40 (br s, 1H), 7.02 (dd, *J* = 8.5, 2 Hz, 1H), 6.77 (d, *J* = 8.5 Hz, 1H), 6.51 (s, 2H), 6.51 (d, *J* = 12 Hz, 1H), 6.46 (d, *J* = 12 Hz, 1H), 3.91 (s, 3H), 3.80 (s, 3H), 3.70 (s, 6H); ^{13}C NMR (C) 152.9 (x 2), 150.7, 150.6*, 147.0*, 137.2,

132.7, 131.8 (center point of quadruplet with $^{2}J_{C-F}$ ~ 33 Hz), 130.4, 126.4, 123.5 (center point of quadruplet with $^{1}J_{C-F}$ ~ 270 Hz), (CH) 129.9, 129.4, 129.3, 125.1, 124.3, 122.2 (quadruplet with $^{3}J_{C-F}$ ~ 4 Hz), 119.3*, 118.8 (quadruplet with $^{3}J_{C-F}$ ~ 4 Hz), 109.7, 106.1 (x 2), (CH_3) 60.8, 55.9 (x 2), 55.8 (starred signals are low and broad); IR ν_{max} (cm^{-1}) 3425 (N−H), 1753 (C=O); HR ESMS *m/z* 526.1452 $[M+Na]^+$. Calc. for $C_{26}H_{24}F_3NNaO_6$, 526.1453.

4-(Trifluoromethyl)phenyl (*Z*)-(2-methoxy-5-(3,4,5-trimethoxystyryl)phenyl)carbamate (19): off-white solid, m. p. 138-141ºC; ^{1}H NMR (500 MHz, $CDCl_3$) δ 8.07 (br s, 1H), 7.66 (apparent d, *J* = 7.5 Hz, 2H), 7.55 (br s, 1H, NH), 7.32 (apparent d, *J* = 7.5 Hz, 2H), 7.03 (d, *J* = 8.5 Hz, 1H), 6.78 (d, *J* = 8.5 Hz, 1H), 6.52 (s, 2H), 6.51 (d, *J* ≈ 12 Hz, 1H), 6.46 (d, *J* = 12 Hz, 1H), 3.91 (s, 3H), 3.81 (s, 3H), 3.71 (s, 6H); ^{13}C NMR (C) 153.2, 152.9 (x 2), 150.5*, 147.0*, 137.3, 132.7, 130.4, 127.7 (center point of quadruplet with $^{2}J_{C-F}$ ~ 32 Hz), 126.4, 123.8 (center point of quadruplet with $^{1}J_{C-F}$ ~ 270 Hz), (CH) 129.4 (x 2), 126.6 (x 2) (quadruplet with $^{3}J_{C-F}$ ~ 4 Hz), 124.3, 121.9 (x 2), 119.4*, 109.7, 106.1 (x 2), (CH_3) 60.8, 55.9 (x 2), 55.8 (starred signals are low and broad); IR ν_{max} (cm^{-1}) 3426 (N−H), 1751 (C=O); HR ESMS *m/z* 526.1448 $[M+Na]^+$. Calc. for $C_{26}H_{24}F_3NNaO_6$, 526.1453.

2,6-Dimethylphenyl (*Z*)-(2-methoxy-5-(3,4,5-trimethoxystyryl)phenyl)carbamate (20): off-white solid, m. p. 109-111ºC; ^{1}H NMR (500 MHz, $CDCl_3$) δ 8.15 (br s, 1H), 7.60 (br s, 1H, NH), 7.07 (br s, 3H), 7.00 (dd, *J* = 8.5, 1.5 Hz, 1H), 6.77 (d, *J* = 8.5 Hz, 1H), 6.53 (s, 2H), 6.49 (d, *J* = 12 Hz, 1H), 6.44 (d, *J* = 12 Hz, 1H), 3.91 (s, 3H), 3.78 (s, 3H), 3.70 (s, 6H), 2.23 (s, 6H); ^{13}C NMR (C) 152.9 (x 2), 150.8*, 147.7, 146.8*, 137.2, 132.7, 130.9 (x 2), 130.3, 127.0, (CH) 129.5, 129.2, 128.5 (x 2), 125.8, 123.8, 119.0*, 109.6, 106.1 (x 2), (CH_3) 60.8, 55.9 (x 2), 55.8, 16.2 (x 2) (starred signals are low and broad); IR ν_{max} (cm^{-1}) 3426 (N−H), 1749 (C=O); HR ESMS *m/z* 486.1891 $[M+Na]^+$. Calc. for $C_{27}H_{29}NNaO_6$, 486.1893.

3,5-Dimethylphenyl (*Z*)-(2-methoxy-5-(3,4,5-trimethoxystyryl)phenyl)carbamate (21): viscous oil; ^{1}H NMR (500 MHz, $CDCl_3$) δ 8.10 (br s, 1H), 7.50 (br s, 1H, NH), 7.00 (dd, *J* = 8.5, 1.5 Hz, 1H), 6.88 (br s, 1H), 6.80 (br s, 2H), 6.75 (d, *J* = 8.5 Hz, 1H), 6.52 (s, 2H), 6.50 (d, *J* = 12 Hz, 1H), 6.44 (d, *J* = 12 Hz, 1H), 3.89 (s, 3H), 3.81 (s, 3H), 3.70 (s, 6H), 2.33 (s, 6H); ^{13}C NMR (C) 152.9 (x 2), 151.6*, 150.5, 146.8*, 139.2 (x 2), 137.2*, 132.8, 130.4, 127.0, (CH) 129.6, 129.2, 127.3, 123.8, 119.3,* 119.2 (x 2), 109.6, 106.1 (x 2), (CH_3) 60.8, 55.9 (x 2), 55.8, 21.2 (x 2) (starred signals are low and broad); IR ν_{max} (cm^{-1}) 3427 (N−H), 1750 (C=O); HR ESMS *m/z* 486.1898 $[M+Na]^+$. Calc. for $C_{27}H_{29}NNaO_6$, 486.1893.

2,3-Dimethylphenyl (*Z*)-(2-methoxy-5-(3,4,5-trimethoxystyryl)phenyl)carbamate (22): yellowish solid, m. p. 136-138ºC; ^{1}H NMR (500 MHz, $CDCl_3$) δ 8.13 (br s, 1H), 7.56 (br s, 1H, NH), 7.11 (br t, *J* = 7.6 Hz, 1H), 7.06 (br d, *J* = 7.6, Hz, 1H), 7.00 (d, *J* = 8.5 Hz, 1H), 6.95 (d, *J* = 7.6 Hz, 1H), 6.76 (d, *J* = 8.5 Hz, 1H), 6.52 (s, 2H), 6.49 (d, *J* = 12 Hz, 1H), 6.44 (d, *J* = 12 Hz, 1H), 3.91 (s, 3H), 3.80 (s, 3H), 3.70 (s, 6H), 2.32 (s, 3H), 2.16 (s, 3H); ^{13}C NMR (C) 152.9 (x 2), 151.5*, 148.9, 146.8*, 138.4, 137.2, 132.7, 130.3, 129.3, 127.1, (CH) 129.6, 129.2, 127.4, 126.0, 123.8, 119.7, 119.2*, 109.6, 106.1 (x 2), (CH_3) 60.8, 55.9 (x 2), 55.8, 20.0, 12.3 (starred signals are low and broad); IR ν_{max} (cm^{-1}) 3424 (N−H), 1750 (C=O); HR ESMS *m/z* 486.1889 $[M+Na]^+$. Calc. for $C_{27}H_{29}NNaO_6$, 486.1893.

3,4-Dimethylphenyl (*Z*)-(2-methoxy-5-(3,4,5-trimethoxystyryl)phenyl)carbamate (23): viscous oil; ^{1}H NMR (500 MHz, $CDCl_3$) δ 8.10 (br s, 1H), 7.50 (br s, 1H, NH), 7.13 (d, *J* = 8 Hz, 1H), 6.99 (d, *J* = 8.5 Hz, 1H), 6.96 (br s, 1H), 6.90 (d, *J* = 8 Hz, 1H), 6.75 (d, *J* = 8.5 Hz, 1H), 6.52 (s, 2H), 6.50 (d, *J* = 12 Hz, 1H), 6.44 (d, *J* = 12 Hz, 1H), 3.89 (s, 3H), 3.81 (s, 3H), 3.70 (s, 6H), 2.27 (s, 3H), 2.25 (s, 3H); ^{13}C NMR (C) 152.9 (x 2), 151.8*, 148.5, 146.8*, 137.7, 137.2, 133.9, 132.8, 130.4, 127.0, (CH) 130.2, 129.7, 129.2, 123.8, 122.6, 119.3*, 118.7, 109.6, 106.1 (x 2), (CH_3) 60.8, 55.9 (x 2), 55.8, 19.8, 19.1

(starred signals are low and broad); IR ν_{max} (cm^{-1}) 3427 (N−H), 1750 (C=O); HR ESMS *m/z* 486.1896 $[M+Na]^+$. Calc. for $C_{27}H_{29}NNaO_6$, 486.1893.

3-Chloro-2-methylphenyl (*Z*)-(2-methoxy-5-(3,4,5-trimethoxystyryl)phenyl)carbamate (24): off-white solid, m. p. 130-132ºC; ^{1}H NMR (500 MHz, $CDCl_3$) δ 8.10 (br s, 1H), 7.60 (br s, 1H, NH), 7.27 (d, *J* = 8 Hz, 1H), 7.15 (t, *J* = 8 Hz, 1H), 7.05-7.00 (m, 2H), 6.77 (d, *J* = 8.5 Hz, 1H), 6.52 (s, 2H), 6.50 (d, *J* = 12 Hz, 1H), 6.45 (d, *J* = 12 Hz, 1H), 3.90 (s, 3H), 3.79 (s, 3H), 3.70 (s, 6H), 2.30 (s, 3H); ^{13}C NMR (C) 152.9 (x 2), 150.8*, 149.6, 146.8*, 137.2, 135.3, 132.6, 130.3, 129.7, 126.6, (CH) 129.4, 129.3, 126.7, 126.6, 124.1, 120.8, 119.2*, 109.6, 106.1 (x 2), (CH_3) 60.8, 55.9 (x 2), 55.8, 13.3 (starred signals are low and broad); IR ν_{max} (cm^{-1}) 3424 (N−H), 1751 (C=O); HR ESMS *m/z* 506.1354 $[M+Na]^+$. Calc. for $C_{26}H_{26}O_6NNaCl$, 506.1346.

4-Chloro-3-methylphenyl (*Z*)-(2-methoxy-5-(3,4,5-trimethoxystyryl)phenyl)carbamate (25): viscous oil; ^{1}H NMR (500 MHz, $CDCl_3$) δ 8.06 (br s, 1H), 7.50 (br s, 1H, NH), 7.33 (d, *J* = 8.8 Hz, 1H), 7.08 (s, 1H), 7.01 (d, *J* = 8.8 Hz, 1H), 6.96 (d, *J* = 8.5 Hz, 1H), 6.76 (d, *J* = 8.5 Hz, 1H), 6.51 (s, 2H), 6.50 (d, *J* = 12 Hz, 1H), 6.45 (d, *J* = 12 Hz, 1H), 3.89 (s, 3H), 3.81 (s, 3H), 3.70 (s, 6H), 2.38 (s, 3H); ^{13}C NMR (C) 152.9 (x 2), 151.2*, 148.9, 146.9*, 137.3, 137.2*, 132.7, 131.1*, 130.4, 126.7, (CH) 129.6, 129.5, 129.3, 124.1, 124.0, 120.3, 119.3*, 109.7, 106.1 (x 2), (CH_3) 60.8, 55.9 (x 2), 55.8, 20.1 (starred signals are low and broad); IR ν_{max} (cm^{-1}) 3424 (N−H), 1751 (C=O); HR ESMS *m/z* 506.1340 $[M+Na]^+$. Calc. for $C_{26}H_{26}O_6NNaCl$, 506.1346.

3-Chloro-4-methylphenyl (*Z*)-(2-methoxy-5-(3,4,5-trimethoxystyryl)phenyl)carbamate (26): viscous oil; ^{1}H NMR (500 MHz, $CDCl_3$) δ 8.06 (br s, 1H), 7.50 (br s, 1H, NH), 7.22 (m, 2H), 7.00 (m, 2H), 6.75 (d, *J* = 8.5 Hz, 1H), 6.51 (s, 2H), 6.50 (d, *J* = 12 Hz, 1H), 6.46 (d, *J* = 12 Hz, 1H), 3.90 (s, 3H), 3.81 (s, 3H), 3.70 (s, 6H), 2.37 (s, 3H); ^{13}C NMR (C) 152.9 (x 2), 151.1*, 148.9, 146.9*, 136.3, 134.4, 133.4, 132.7, 130.4, 126.7, (CH) 131.0, 129.5, 129.3, 124.1, 122.4, 119.9*, 119.4, 109.7, 106.1 (x 2),

(CH_3) 60.9, 55.9 (x 2), 55.8, 19.4 (starred signals are low and broad); IR ν_{max} (cm^{-1}) 3425 (N−H), 1752 (C=O); HR ESMS *m/z* 506.1350 $[M+Na]^+$. Calc. for $C_{26}H_{26}O_6NNaCl$, 506.1346.

5.2. Biological studies. Materials and methods

5.2.1. Cell culture

Cell culture media were purchased from Gibco (Grand Island, NY). Fetal bovine serum (FBS) was obtained from Harlan-Seralab (Belton, U.K.). Supplements and other chemicals not listed in this section were obtained from Sigma Chemical Co. (St. Louis, MO). Plastics for cell culture were supplied by Thermo Scientific BioLite. All tested compounds were dissolved in DMSO at a concentration of 10 mM and stored at −20°C until use.

HT-29, MCF-7, HeLa, A549, MDA-MB-231, HL-60 and HEK-293 cell lines were maintained in Dulbecco's modified Eagle's medium (DMEM) containing glucose (1 g/L), glutamine (2 mM), penicillin (50 μg/mL), streptomycin (50 μg/mL), and amphotericin B (1.25 μg/mL), supplemented with 10% FBS. HMEC-1 cell line was maintained in Dulbecco's modified Eagle's medium (DMEM)/Low glucose containing glutamine (2 mM), penicillin (50 μg/mL), streptomycin (50 μg/mL), and amphotericin B (1.25 μg/mL), supplemented with 10% FBS. For the development of tube formation assays in Matrigel, HMEC-1 cells were cultured in EGM-2MV Medium supplemented with EGM-2MV SingleQuots.

5.2.2. Cell proliferation assay

In 96-well plates, 3×10^3 (HeLa, A549, HMEC-1, HEK-293), 5×10^3 (HT-29, MCF-7) or 1×10^4 (HL-60) cells per well were incubated with serial dilutions of the tested compounds in a total volume of 100 μL of their respective growth media. The 3-(4,5-dimethylthiazol-2-yl)-2,5-diphenyltetrazolium

bromide (MTT; Sigma Chemical Co.) dye reduction assay in 96-well microplates was used, as previously described [18]. After 2 days of incubation (37 °C, 5% CO_2 in a humid atmosphere), 10 µL of MTT (5 mg/mL in phosphate-buffered saline, PBS) was added to each well, and the plate was incubated for a further 3 h (37 °C). For adherent cells, the supernatant was discarded and replaced by 100 µL of DMSO to dissolve formazan crystals. For non-adherent cells (HL-60), plates are centrifugated at 800 rpm for 5 min before discarding the supernatant. The absorbance was then read at 540 nm by spectrophotometry. Three independent experiments were performed, and the IC_{50} values (i.e., concentration half inhibiting cell proliferation) were graphically determined using GraphPad Prism 4 software.

In the case of MDA-MB-231 cells, 1×10^4 cells per well were seeded in 48-well plates in 1 mL of growth medium. One day later, 5-fold dilutions of the compounds were added. After 3 days of incubation, cells were trypsinized and counted in a Coulter counter (Rega Institute for Medical Research, KU Leuven). The IC_{50} value was determined as the compound concentration required to reduce cell proliferation by 50%.

5.2.3. Tubulin self-assembly assay

Purified tubulin was used for these measurements. Tubulin polymerization was carried out in a 96 well-plate. In each well 50 µL of a solution of 25 µM of tubulin in GAB buffer was added to 50 µL of 27.5 µM solution of the corresponding compounds in GAB buffer (20 mM sodium phosphate, 10 mM $MgCl_2$, 1 mM EGTA, 30% glycerol) and 0.1 mM GTP at pH = 6.5. Then, the plate was incubated at 37ºC in Multiskan® and absorbance at 340 nM was registered every 30 seconds during 2 hours.

5.2.4. EBI assay

MDA-MB-231 cells were seeded in 6-well plates at 5×10^5 cells per well. After 48 h, compounds were added to the cells for 16 h before adding EBI (N, N'-ethylene-bis(iodoacetamide)) at 100 µM. After 1.5 h, cells were harvested and cell extracts were prepared for Western Blot analysis. Thirty µg of

proteins were subjected to gel electrophoresis using 0.1% SDS (85% purity) and 10% polyacrylamide gels. After electrophoresis, proteins were transferred to pretreated Hybond-P polyvinylidene difluoride (PVDF) membranes, which were incubated overnight at 4ºC in blocking buffer (2.5% non-fat dry milk in PBS containing 0.1% Tween) and subsequently for 1 h at rt in blocking buffer primary antibody raised against β-tubulin. After washing, membranes were incubated with the corresponding HRP-conjugated secondary antibody in blocking buffer for 30 min at rt. Next, membranes were washed extensively and immunoreactive proteins were detected by chemiluminiscence (ECLplus, Bio-Rad).

5.2.5. Cell cycle analysis

Progression of the cell cycle was analysed by means of flow cytometry with propidium iodide. After incubation with compounds for 24 h, A549 cells were fixed, treated with RNase and stained with propidium iodide following instructions of BD Cycletest^{TM} DNA Kit. Analysis was performed with a BD Accuri^{TM} C6 flow cytometer.

5.2.6. Immunofluorescence assay

Immunofluorescent analysis of the microtubule network was performed on the A-549 cell line. In this assay, 1,5x10^5 cells were plated on a coverglass and incubated with the different concentrations of selected compounds for 16 h. Cells were then washed with PEMP, permeabilized with PEM-Triton X-100 0.5% for 90 seconds at room temperature and fixed in 3.7% formaldehyde (in PEM pH 7.4) for 30 min at rt. Direct immunostaining was carried out for 2.5 h at 37°C in darkness with primary FITC-conjugated anti-α-tubulin antibody (dilution 1:400 in PBS-BSA 1% from a 1 mg/mL solution; monoclonal antibody, clone DM1A, Sigma-Aldrich). Next, cells were washed with PBS and incubated for 30 min at room temperature in darkness with Hoechst 2 mM in water. Then, cells were washed in PBS and coverglasses were mounted with 10 μL of Glycine/Glycerol buffer. The cytoskeleton was imaged by a confocal laser scanning microscope (CLSM) Leica SP5 with a Leica inverted microscope,

equipped with a Plan-Apochromat 63× oil immersion objective (NA=1.4). Each image was recorded with the CLSM's spectral mode selecting specific domains of the emission spectrum. The FITC fluorophore was excited at 488 nm with an argon laser and its fluorescence emission was collected between 496 nm and 535 nm.

5.2.7. Apoptosis assay

Apoptosis was determined by quantifying FITC-Annexin V translocation by means of flow cytometry. A549 cells were incubated with compounds for 24 h and then stained following instructions of BD Apoptosis Detection™ Kit. Analysis was performed with a BD Accuri™ C6 flow cytometer.

5.2.8. Tube destruction assay

Wells of a 96-well μ-plate for angiogenesis were coated with 12 μL of Matrigel (10 mg/mL, BD Biosciences) at 4ºC. After gelatinization at 37ºC for 30 min, HMEC-1 cells were seeded at 2 x 10^4 cells/well in 35 μL of culture medium on top of the Matrigel. After 20 h of incubation at 37ºC, when tube-like structures were detectable, compounds were added at different concentrations. Next, 4 h later, tube destruction was evaluated by giving a score from 0 to 3 (3: intact tubular network as seen in the control, 2: missing connections and/or dead ends; 1: many separate small tubes that are not connected; 0: no tubes).

5.2.9. Proteins and ligands

Calf brain tubulin was purified as described previously [19].

Acknowledgments

This research has been funded by the Ministerio de Economía y Competitividad (project CTQ2014-52949-P), by the Universitat Jaume I (project PI-1B2015-75) and by the Conselleria d'Educació, Investigació, Cultura i Sport de la Generalitat Valenciana (project PROMETEO 2013/027). L. C-M. thanks spanish Ministry of Education, Culture and Sport for a FPU fellowship (FPU14/00878). The

authors are also grateful to the SCIC of the Universitat Jaume I for providing NMR and Mass Spectrometry facilities.

Supplementary Information

Additional NMR data of all new synthetic compounds are provided in the Supplementary Information.

References

[1] R. Ronca, M. Benkheil, S. Mitola, S. Struyf, S. Liekens, Tumor angiogenesis revisited: Regulators and clinical implications. *Med. Res. Rev.* **2017**. doi: 10.1002/med.21452.

[2] (a) G. M. Tozer, C. Kanthou, B. C. Bagule, Disrupting tumour blood vessels. *Nat. Rev. Cancer* **2005**, *5*, 423-435. (b) M. M. Mita, Sargsyan, L.; A. C. Mita, M. Spear, Vascular-disrupting agents in oncology. *Expert Opin. Investig. Drugs* **2013**, *22*, 317-328. (c) M-J. Pérez-Pérez, E-M. Priego, O. Bueno, M. S. Martins, M-D. Canela, S. Liekens, Blocking blood flow to solid tumors by destabilizing tubulin: an approach to targeting tumor growth. *J. Med. Chem*. **2016**, *59*, 8685-8711.

[3] G. R.; Pettit, S. B. Singh, M. R. Boyd, E. Hamel, R. K. Pettit, J. M. Schmidt, F. Hogan, Antineoplastic agents. 291. Isolation and synthesis of combretastatins A-4, A-5, and A-6. *J. Med. Chem.* **1995**, *38*, 1666–1672.

[4] M. Su, J. Huang, S. Liu, Y. Xiao, X. Qin, J. Liu, C. Pi, T. Luo, J. Li, X. Chen, Z. Luo, The anti-angiogenic effect and novel mechanisms of action of Combretastatin A-4. *Sci. Rep.* **2016**, DOI: 10.1038/srep28139.

[5] L. M. Greene, M. J. Meegan, D. M. Zisterer, Combretastatins: More Than Just Vascular Targeting Agents? *J. Pharmacol. Exp. Ther.* **2015**, *355*, 212–227.

[6] (a) D. W. Siemann, D. J. Chaplin, P. A. Walicke, A review and update of the current status of the vasculature disabling agent combretastatin-A 4 phosphate (CA4P). *Expert Opin. Investig. Drugs.* **2009**, *18*, 189-197. (b) G. Nagaiah, S. C. Remick, Combretastatin A4 phosphate: a novel vascular disrupting agent. *Future Oncol.* **2010**, *6*, 1219-1228.

[7] (a) P. Hinnen, F. Eskens, Vascular disrupting agents in clinical development. *Br. J. Cancer* **2007**, *96*, 1159-1165. (b) M. A. Spear, P. LoRusso, A. Mita, M. Mita, Vascular Disrupting Agents (VDA) in Oncology: Advancing Towards New Therapeutic Paradigms in the Clinic. *Curr. Drug Targets* **2011**, *12*, 2009-2015. For recent studies on combretastatin derivatives see: (a) M. Mustafa, D. Abdelhamid, E. M.N. Abdelhafez, M. A. A.Ibrahim, A. M. Gamal-Eldeen, O. M. Alya, Synthesis, antiproliferative, anti-tubulin activity, and docking study of new 1,2,4-triazoles as potential combretastatin analogues. *Eur. J. Med. Chem.* **2017**, *141*, 293-305. (b) A. M. Malebari, L. M. Greene, S. M. Nathwani, D. Fayne, N. M. O'Boyle, S. Wang, B. Twamley, D. M. Zisterer, M. J. Meegan, β-Lactam analogues of combretastatin A-4 prevent metabolic inactivation by glucuronidation in chemoresistant HT-29 colon cancer cells. *Eur. J. Med. Chem.* **2017**, *130*, 261-285. (c) Y. H. Li, B. Zhang, H. K. Yang, Q. Li, P. C. Diao, W. W. You, P. L. Zhao, Design, synthesis, and biological evaluation of novel alkylsulfanyl-1,2,4-triazoles as cis-restricted combretastatin A-4 analogues. *Eur. J. Med. Chem.* **2017**, *125*, 1098-1106.

[8] K. Ohsumi, R. Nakagawa, Y. Fukuda, T. Hatanaka, Y. Morinaga, Y. Nihei, K. Ohishi, Y. Suga, Y. Akiyama, T. Tsuji, Novel combretastatin analogues effective against murine solid tumors: design and structure-activity relationships. *J. Med. Chem*. **1998**, *41*, 3022-3032. For studies on aminocombretastatin derivatives see: (a) J-Y. Chang, M-F. Yang, C-Y. Chang, C-M. Chen, C-C. Kuo, J-P. Liou, 2-Amino and 2-aminocombretastatin derivatives as potent antimitotic agents. *J. Med. Chem.* **2006**, *49*, 6412-6415. (b) A. Kamala, B. Shaika, V. L. Nayaka, B. Nagaraju, J. S. Kapure, M. S. Malika, T. B. Shaika, B. Prasad, Synthesis and biological evaluation of 1,2,3-triazole linked

aminocombretastatin conjugates as mitochondrial mediated apoptosis inducers. *Bioorg. Med. Chem*. **2014**, *22*, 5155-5167.

[9] A. K. Ghosh, M. Brindisi, Organic Carbamates in Drug Design and Medicinal Chemistry. *J. Med. Chem.* **2015**, *58*, 2895-2940.

[10] (a) A. Delmonte, C. Sessa, AVE8062: a new combretastatin derivative vascular disrupting agent. *Expert Opin. Investig. Drugs.* **2009**, *18*, 1541-1548. (b) D. Durrant, F. Corwin, D. Simoni, M. Zhao, M. A. Rudek, F. N.·Salloum, R. C. Kukreja, P. P. Fatouros, R. Lee, M. cis-3, 4´, 5-Trimethoxy-3´-aminostilbene disrupts tumor vascular perfusion without damaging normal organ perfusion. *Cancer Chemother. Pharmacol.* **2009**, *63*, 191–200. (c) G. Nagaiah, S. C. Remick. Combretastatin A4 phosphate: a novel vascular disrupting agent. *Future Oncol.* **2010**, *6*, 1219–1228.

[11] C. Vilanova, S. Díaz-Oltra, J. Murga, E. Falomir, M. Carda, M. Redondo-Horcajo, J. F. Díaz, I. Barasoain, J. A. Marco, Design and synthesis of pironetin analogue/colchicine hybrids and study of their cytotoxic activity and mechanisms of interaction with tubulin. *J. Med. Chem*. **2014**, *57*, 10391-10403.

[12] (a) S. Torijano-Gutiérrez, S. Díaz-Oltra, E. Falomir, J. Murga, M. Carda, J. A. Marco, Synthesis of combretastatin A-4 O-alkyl derivatives and evaluation of their cytotoxic, antiangiogenic and antitelomerase activity. *Bioorg. Med. Chem*. **2013**, *21*, 7267-7274. (b) C. Vilanova, S. Torijano-Gutiérrez, S. Díaz-Oltra, J. Murga, E. Falomir, M. Carda, J. A. Marco, Design and synthesis of pironetin analogue/combretastatin A-4 hybrids containing a 1,2,3-triazole ring and evaluation of their cytotoxic activity. *Eur. J. Med. Chem*. **2014**, *87*, 125-130. (c) S. Torijano-Gutiérrez, C. Vilanova, S. Díaz-Oltra, J. Murga, E. Falomir, M. Carda, J A. Marco, Design and synthesis of pironetin analogue/combretastatin A-4 hybrids and evaluation of their cytotoxic activity. *Eur. J. Org. Chem*. **2014**, 2284-2296.

[13] (a) D. Simoni, F. P. Invidiata, M. Eleopra, P. Marchetti, R. Rondanin, R. Baruchello, G. Grisolia, A. Tripathi, G. E. Kellogg, D. Durrant, R. M. Lee, Design, synthesis and biological evaluation of novel stilbene-based antitumor agents. *Bioorg. Med. Chem.* **2009**, *17*, 512-522. (b) M. S. Gerova, S. R. Stateva, E. M. Radonova, R. B. Kalenderska, R. I. Rusew, R. P. Nikolova, C. D. Chanev, B. L. Shivachev, M. D. Apostolova, O. I. Petrov, Combretastatin A-4 analogues with benzoxazolone scaffold: Synthesis, structure and biological activity. *Eur. J. Med. Chem.* **2016**, *120*, 121-133.

[14] Y-Q. Liu, X-J. Li, C-Y. Zhao, X. Nan, et al., Synthesis and mechanistic studies of novel spin-labeled combretastatin derivatives as potential antineoplastic agents. *Bioorg. Med. Chem.* **2013**, *21*, 1248-1256.

[15] L. Zhang, W. Xia, B. Wang, Y. Luo, W. Lu, Convenient synthesis of sorafenib and its derivatives. *Synth. Commun.* **2011**, *41*, 3140-3146.

[16] L. Yang, G. Li, S. Ma, C. Zou, S. Zhou, Q. Sun, C. Cheng, X. Chen, L. Wang, S. Feng, L. Li, S. Yang, Structure-activity relationship studies of pyrazolo[3,4-d]pyrimidine derivatives leading to the discovery of a novel multikinase inhibitor that potently inhibits FLT3 and VEGFR2 and evaluation of its activity against acute myeloid leukemia in vitro and in vivo. *J. Med. Chem.* **2013**, *56*, 1641-1655.

[17] S. Fortin, J. Lacroix, M.-F. Côté, É. Petitclerc, R. C. Gaudreault, Quick and Simple Detection Technique to Assess the Binding of Antimicrotubule Agents to the Colchicine-Binding Site *Biol. Proced. Online* **2010**, *12*, 113–117.

[18] S. Rodríguez-Nieto, M. A. Medina, A.R. Quesada, A re-evaluation of fumagillin selectivity towards endothelial cells. *Anticancer Research* **2001**, *21*, 3457-3460.

[19] J. M. Andreu, Large scale purification of brain tubulin with the modified Weisenberg procedure. *Methods Mol. Med.* **2007**, *137*, 17-28.

List of captions

Figure 1.

Figure 2.

Scheme 1. Reagents and conditions**:** Method a: ArOCOCl, pyridine, THF, 0ºC 30 min then rt 1 h. Method b: (i) Triphosgene, Et_3N, THF, rt, 10 min; (ii) ArOH, THF, 45ºC, 1 h.

Figure 3. Structure of the carbamates investigated in this study..

Table 1. IC_{50} values (nM) for CA-4, AmCA-4 and derivatives **1**-**26**.[a]

Table 2. Critical Concentration (CrC) for the assembly of purified tubulin in GAB in the presence of CA-4, AmCA-4 or the carbamates.

Figure 4. Effects of CA-4, AmCA-4 and carbamates on the in vitro tubulin polymerization.

Figure 5. Effects of colchicine and carbamates at the colchicine-binding site of tubulin.

Table 3. Cell cycle distribution (%).

Figure 6. Effects of AmCA-4 and some selected carbamates on the microtubule network. A549 cells were treated for 16 hours and processed for immunofluorescence microscopy: (A) DMSO, (B) 230 nM AmCA-4, (C) 150 nM compound **1**, (D) 300 nM compound **3**, (E) 260 nM compound **5**, (F) 200 nM compound **6**, (G) 220 nM compound **17** and (H) 260 nM compound **18**.

Figure 7. Apoptotic effect of AmCA-4 and carbamates. Data are the average (±SD) of three experiments.

Figure 8. Tube destruction effect of selected carbamates. All the compounds were tested at 3 μM, 1 μM, 300 nM, 30 nM, 10 nM and 3 nM

Figure 9. Effect of carbamate **25** on the tubular network. (A) 3 nM, (B) 10 nM, (C) 30 nM, (D) 100 nM.

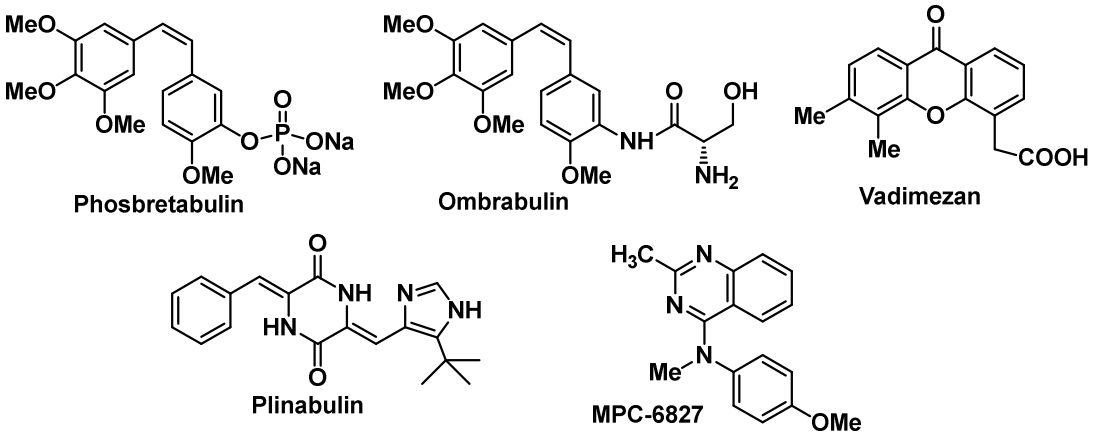
MeO
MeO
OMe
O
P
ONa
ONa
OMe
Phosbretabulin
MeO
MeO
OMe
O
OH
NH
NH2
OMe
Ombrabulin
O
Me
O
Me
COOH
Vadimezan
O
NH
N
NH
HN
O
Plinabulin
H3C
N
N
N
Me
MPC-6827
OMe

Figure 1.

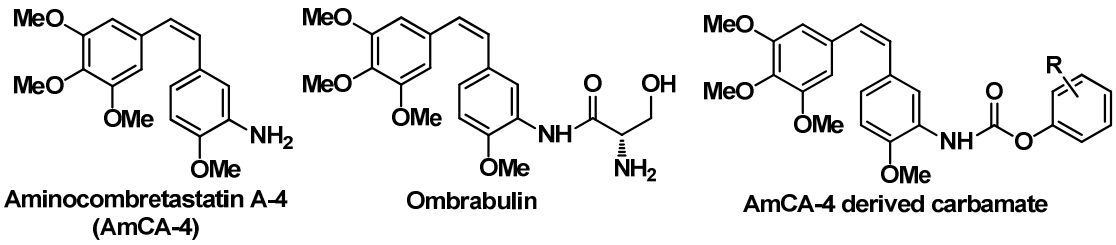
MeO
MeO
OMe
NH2
OMe
Aminocombretastatin A-4
(AmCA-4)
MeO
MeO
OMe
NH
O
OH
OMe
NH2
Ombrabulin
MeO
MeO
OMe
NH
O
O
R
OMe
AmCA-4 derived carbamate

Figure 2.

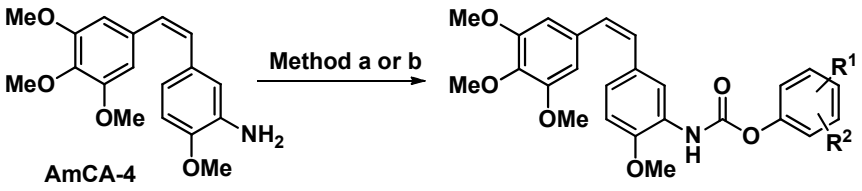
MeO
MeO
OMe
NH2
OMe
AmCA-4
Method a or b
MeO
MeO
OMe
N
H
O
O
OMe
R1
R2

Scheme 1.

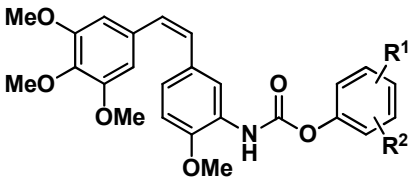

1 (R^1, R^2=H, method a , 89%)
2 (R^1=2-F, R^2=H, method b, 73%)
3 (R^1=3-F, R^2=H, method b, 33%)
4 (R^1=4-F, R^2=H, method a , 64%)
5 (R^1=2-Cl, R^2=H, method b, 35%)
6 (R^1=3-Cl, R^2=H, method b, 33%)
7 (R^1=4-Cl, R^2=H, method a , 62%)
8 (R^1=2-Br, R^2=H, method b, 36%)
9 (R^1=3-Br, R^2=H, method b, 58%)
10 (R^1=4-Br, R^2=H, method b, 61%)
11 (R^1=2-OMe, R^2=H, method b, 41%)
12 (R^1=3-OMe, R^2=H, method b, 91%)
13 (R^1=4-OMe, R^2=H, method b, 73%)
14 (R^1=2-Me, R^2=H, method b , 27%)
15 (R^1=3-Me, R^2=H, method b, 45%)
16 (R^1=4-Me, , R^2=H, method b, 49%)
17 (R^1=2-CF_3, R^2=H, method b , 65%)
18 (R^1=3-CF_3, R^2=H, method b, 50%)
19 (R^1=4-CF_3, R^2=H, method b, 75%)
20 (R^1=2-Me, R^2=6-Me, method b, 24%)
21 (R^1=3-Me, R^2=5-Me, method b, 18%)
22 (R^1=2-Me, R^2=3-Me, method b, 28%)
23 (R^1=3-Me, R^2=4-Me, method b, 27%)
24 (R^1=2-Me, R^2=3-Cl, method b, 55%)
25 (R^1=3-Me, R^2=4-Cl, method b, 31%)
26 (R^1=4-Me, R^2=3-Cl, method b, 24%)

Figure 3.

Table 1.

Comp.	HT-29	MCF-7	HeLa	A549	HL-60	HMEC-1	HEK-293
CA-4	4200 ± 500	1000 ± 200	2100 ± 600	130 ± 20	4000 ± 1000	3400 ± 400	25000 ± 300
AmCA-4	22.0 ± 0.7	8.0 ± 0.9	2.6 ± 0.5	117 ± 7	4.5 ± 0.9	12 ± 6	7.1 ± 1.0
1	2.9 ± 0.5	9.8 ± 0.1	4.8 ± 0.2	77 ± 12	4 ± 2	12 ± 5	3.3 ± 0.2
2	110 ± 30	62 ± 2	17 ± 2	320 ± 190	4 ± 2	180 ± 20	65 ± 4
3	10.6 ± 0.5	7.0 ± 0.6	2.7 ± 1.3	150 ± 40	60 ± 20	20 ± 2	13.2 ± 0.2
4	60 ± 20	95.4 ± 1.3	60 ± 20	400 ± 200	50 ± 30	65 ± 13	185 ± 2
5	17.8 ± 0.7	10.1 ± 0.8	5 ± 2	130 ± 40	3.7 ± 0.7	50 ± 30	41 ± 2
6	9.2 ± 1.3	4.4 ± 0.6	4.79 ± 0.03	100 ± 20	13.5 ± 1.6	9 ± 6	14.5 ± 0.4
7	31 ± 14	82 ± 13	24 ± 3	800 ± 200	770 ± 170	76 ± 13	142 ± 9
8	7.5 ± 0.6	18.9 ± 0.9	2.6±1.0	180 ± 50	3 ± 2	22 ± 7	8 ± 5
9	11.3 ± 0.7	5.9 ± 0.3	2.6±0.5	160 ± 30	5.6 ± 0.6	12 ± 4	16 ± 2
10	3.5 ± 0.2	0.75 ± 0.05	1.2±0.2	150 ± 30	5 ± 3	7 ± 4	19 ± 7
11	290 ± 100	230 ± 180	348 ± 13	3000 ± 1100	350 ± 190	400 ± 15	160 ± 40
12	4.8 ± 0.5	7.18 ± 0.07	3.4 ± 0.4	160 ± 40	4.9 ± 0.5	5 ± 2	8.1 ± 0.2
13	350 ± 20	230 ± 30	200 ± 40	550 ± 120	50 ± 6	120 ± 50	130 ± 40
14	160 ± 70	380 ± 50	50 ± 30	460 ± 110	222 ± 7	55 ± 6	60 ± 20
15	46 ± 3	25 ± 9	23 ± 13	390 ± 180	67 ± 2	50 ± 20	40 ± 20
16	270 ± 80	200 ± 60	370 ± 160	1500 ± 300	52 ± 2	160 ± 40	144 ± 10
17	16 ± 7	44 ± 2	15 ± 4	110 ± 40	6.7 ± 0.6	19 ± 5	4.1 ± 1.0
18	13 ± 3	56 ± 9	40 ± 8	130 ± 60	4 ± 2	16 ± 5	42.2 ± 0.9
19	27.6 ± 0.6	9.2 ± 0.3	21 ± 8	270 ± 70	40 ± 30	30 ± 8	57 ± 22
20	600 ± 200	440 ± 14	320 ± 120	3900 ± 1200	470 ± 70	380 ± 140	490 ± 80
21	260 ± 140	210 ± 20	130 ± 16	1540 ± 80	620 ± 90	180 ± 7	150 ± 80
22	175 ± 4	16 ± 3	40 ± 20	900 ± 200	59 ± 13	140 ± 40	80 ± 30
23	130 ± 20	170 ± 30	21 ± 6	1300 ± 600	69 ± 11	130 ± 50	97 ± 9
24	47 ± 2	39 ± 3	23 ± 12	140 ± 30	70 ± 30	20 ± 2	14 ± 2
25	11.4 ± 0.3	8.1 ± 0.9	3.3 ± 0.5	140 ± 30	0.4 ± 0.2	7 ± 1	8.4 ± 0.6
26	23 ± 2	6.1 ± 0.8	3.7 ± 0.3	90 ± 20	1.8 ± 0.6	6 ± 2	7.0 ± 0.8

[a]IC_{50} values are expressed as the compound concentration (nM) that inhibits the cell growth by 50%. Data are the average (±SD) of three experiments.

Table 2.

Compound	CrC (μM)	Compound	CrC (μM)
Control	8 ± 1	**13**	23 ± 2
CA-4	22 ± 1	**14**	22 ± 3
AmCA-4	23 ± 2	**15**	20 ± 3
1	20 ± 2	**16**	25 ± 2
2	18 ± 3	**17**	23 ± 2
3	24 ± 4	**18**	14 ± 2
4	22 ± 2	**19**	20 ± 3
5	21 ± 3	**20**	17 ± 3
6	23 ± 2	**21**	24 ± 2
7	24 ± 2	**22**	25 ± 2
8	22 ± 2	**23**	21 ± 2
9	25 ± 3	**24**	23 ± 1
10	23 ± 2	**25**	24 ± 3
11	16 ± 1	**26**	24 ± 3
12	20 ± 2		

[a] Data are the average (±SD) of three experiments.

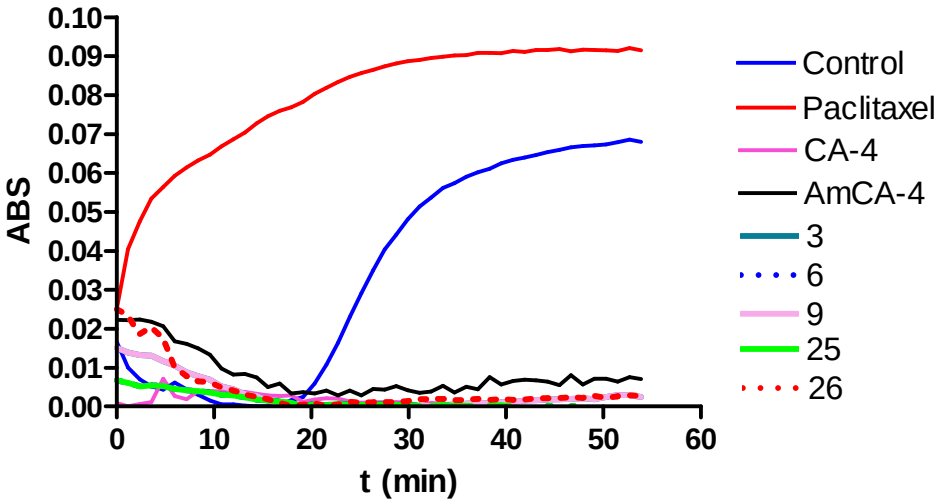
0.10
0.09
0.08
0.07
0.06
0.05
0.04
0.03
0.02
0.01
0.00
ABS
0
10
20
30
40
50
60
t (min)
Control
Paclitaxel
CA-4
AmCA-4
3
6
9
25
26

Figure 4.

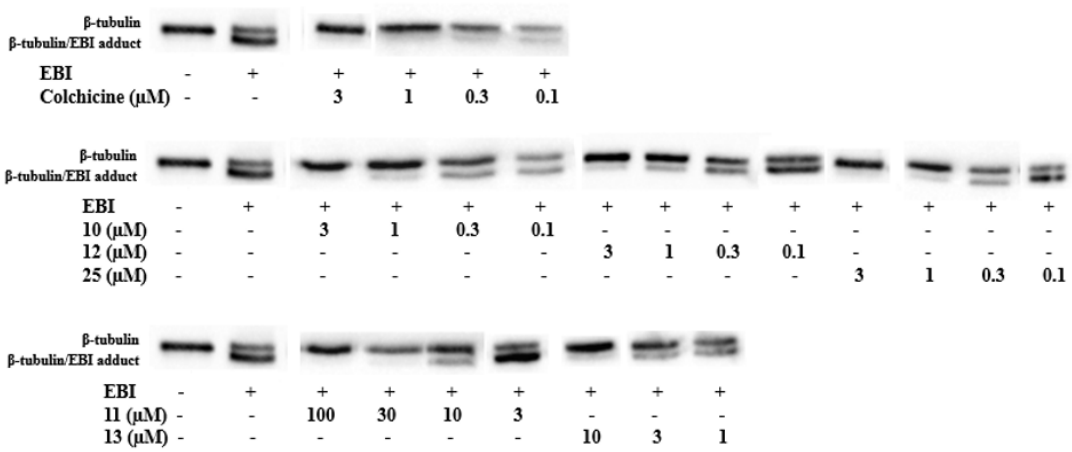
β-tubulin
β-tubulin/EBI adduct
EBI - + + + + +
Colchicine (μM) - - 3 1 0.3 0.1
β-tubulin
β-tubulin/EBI adduct
EBI - + + + + + + + + + + + + +
10 (μM) - - 3 1 0.3 0.1 - - - - - - - -
12 (μM) - - - - - - 3 1 0.3 0.1 - - - -
25 (μM) - - - - - - - - - - 3 1 0.3 0.1
β-tubulin
β-tubulin/EBI adduct
EBI - + + + + + + + +
11 (μM) - - 100 30 10 3 - - -
13 (μM) - - - - - - 10 3 1

Figure 5.

Table 3.

Comp.	Conc (nM)	SubG0	G0/G1	S	G2/M
Control	-	6.6 ± 0.1	66 ± 1	16 ± 1	11 ± 1
CA-4	50	15 ± 1	21 ± 2	22 ± 1	43 ± 1
AmCA-4	60	14 ± 1	21 ± 1	24 ± 1	41 ± 2
1	40	20 ± 3	21 ± 1	15 ± 1	44 ± 3
2	160	17 ± 1	31 ± 3	13 ± 1	39 ± 2
3	75	19 ± 1	29 ± 1	10 ± 1	43 ± 2
4	200	21 ± 1	26 ± 5	19 ± 1	34 ± 1
5	65	16 ± 1	29 ± 2	12 ± 2	43 ± 3
6	50	16 ± 2	30 ± 1	10 ± 1	44 ± 2
7	400	20 ± 1	21 ± 1	18 ± 1	41 ± 1
8	90	17 ± 2	29 ± 1	10 ± 1	44 ± 3
9	80	17 ± 3	30 ± 1	12 ± 1	39 ± 1
10	75	19 ± 1	32 ± 3	17 ± 1	33 ± 1
11	1500	17 ± 1	29 ± 4	12 ± 3	43 ± 1
12	80	17 ± 1	31 ± 1	16 ± 2	36 ± 3
13	275	14 ± 1	25 ± 1	14 ± 1	46 ± 2
14	230	16 ± 1	31 ± 2	13 ± 2	40 ± 1
15	200	22 ± 3	26 ± 2	16 ± 3	36 ± 1
16	750	27 ± 5	24 ± 1	16 ± 2	32 ± 3
17	55	20 ± 2	21 ± 2	15 ± 1	44 ± 5
18	65	16 ± 3	28 ± 1	15 ± 1	41 ± 1
19	135	26 ± 1	22 ± 1	14 ± 1	39 ± 2
20	2000	23 ± 2	25 ± 2	17 ± 1	35 ± 1
21	750	22 ± 3	24 ± 3	16 ± 1	38 ± 1
22	450	12 ± 1	24 ± 1	22 ± 3	42 ± 2
23	650	17 ± 1	24 ± 1	19 ± 1	41 ± 1
24	70	20 ± 1	24 ± 1	18 ± 2	39 ± 1
25	70	18 ± 1	24 ± 1	22 ± 9	36 ± 8
26	45	29 ± 4	21 ± 1	14 ± 1	36 ± 3

[a] Data are the average (±SD) of three experiments.

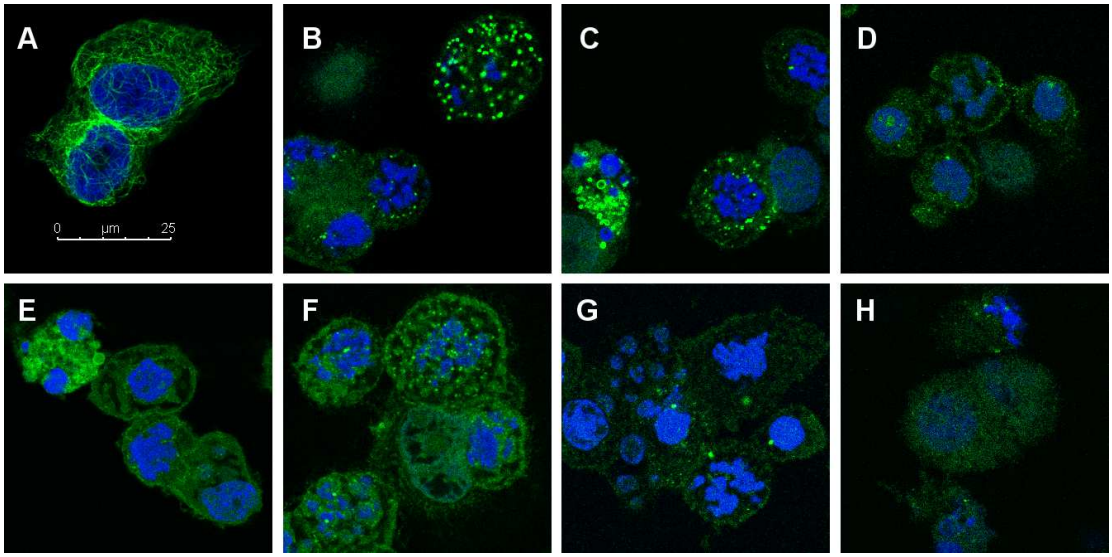

Figure 6.

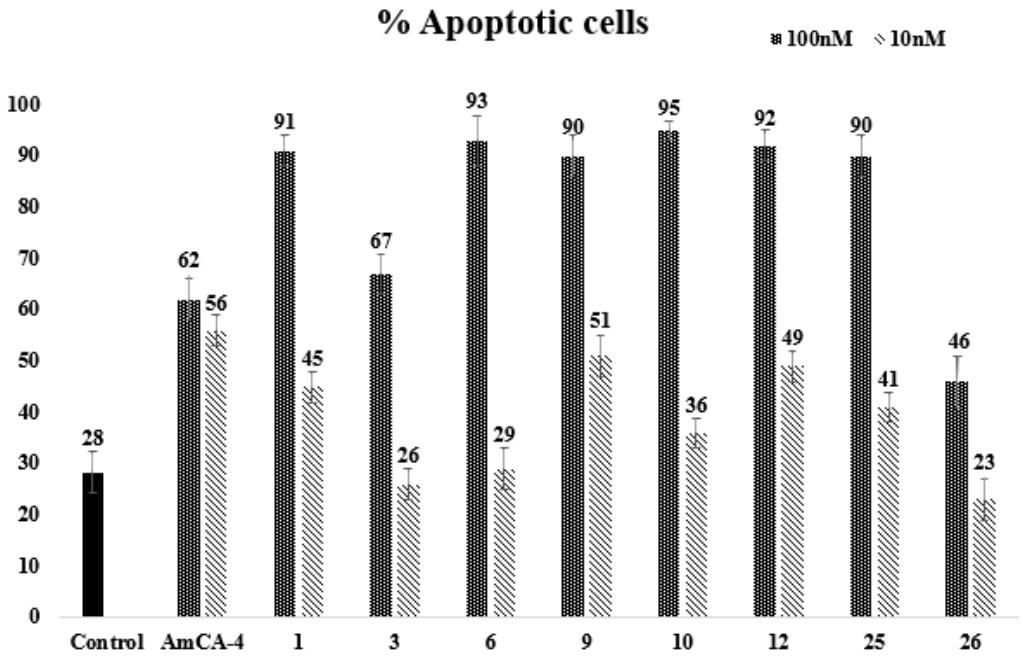
% Apoptotic cells
100nM
10nM
100
90
80
70
60
50
40
30
20
10
0
28
62
56
91
45
67
26
93
29
90
51
95
36
92
49
90
41
46
23
Control
AmCA-4
1
3
6
9
10
12
25
26

Figure 7.

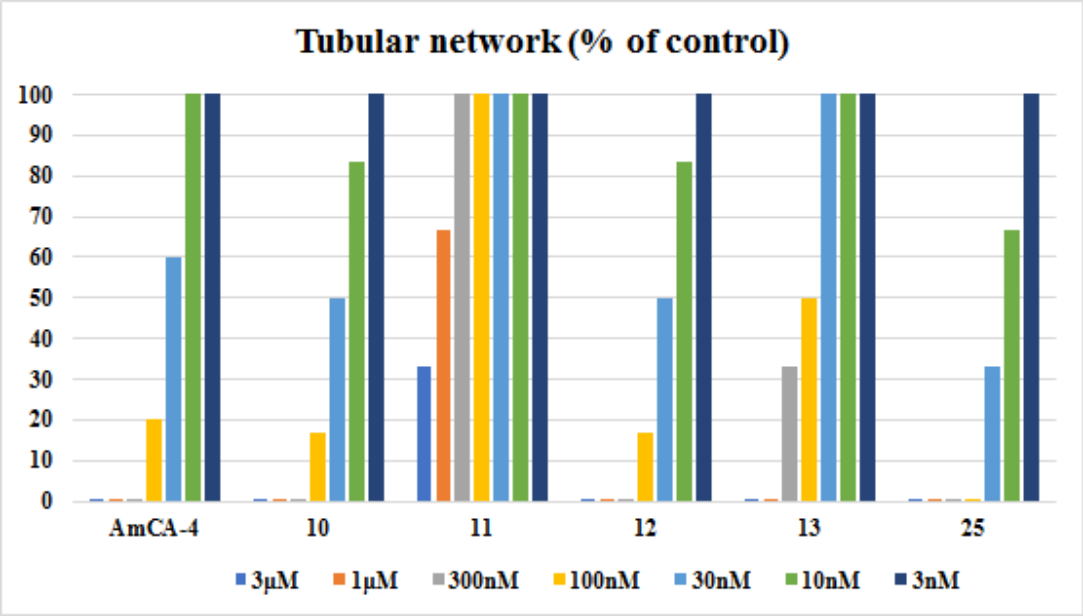
Tubular network (% of control)
100
90
80
70
60
50
40
30
20
10
0
AmCA-4
10
11
12
13
25
3µM
1µM
300nM
100nM
30nM
10nM
3nM

Figure 8.

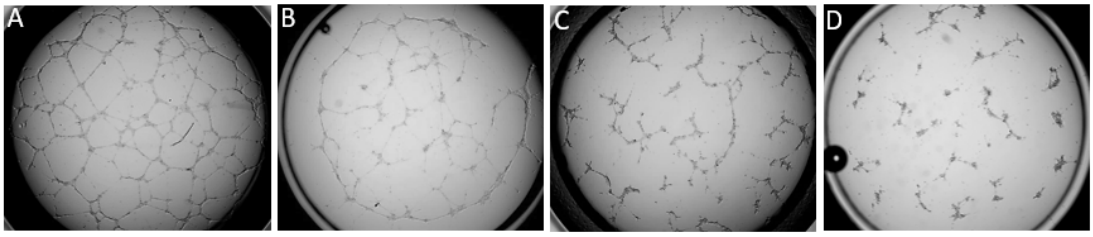

Figure 9.